3D Multiple-point Statistics Simulations of the Roussillon Continental Pliocene Aquifer using DeeSse (Valentin Dall'alba et al)

Hydrol. Earth Syst. Sci. Discuss.,https://doi.org/10.5194/hess-2020-96-RC1, 2020

We appreciate the helpful comments of the reviewers and editor. Please find below in black font, the summary of how we have addressed each reviewer's comments (blue font) in the revised manuscript. The line numbers refer to the revised manuscript.

Answer to Referee #1 :

General comments :

This manuscript provides an improvement of the MPS implementation through the direct sampling algorithm, in order to design a method for the reconstruction of aquifer heterogeneity at scale lengths of tens of kilometers.

More precisely, the aim of the paper is to present a workflow allowing to apply the direct sampling technique to simulate aquifer heterogeneity at the regional scale. We do not improve the actual implementation of the MPS kernel. We employ the direct sampling MPS kernel into a global workflow.

Overall, the work is interesting and deserves publication. The paper is generally well organized and written, but it can be improved following the suggestions given in the specific comments # 1 and 6. Some other weak scientific flaws can be fixed with a moderate to major revision.

We are thankful to the reviewer for his/her overall evaluation and detailed editing of the paper. This is helping to improve the manuscript and clarify some aspects. Below we discuss more precisely the different issues raised by the reviewer and how we have adjusted the paper in consequence.

Specific comments :

The abstract is a long summary of the work, but it does not give a precise and clear image of the innovative content of the work. I think that it should be shortened and focused in a more appropriate way.

We agree that the abstract was long and maybe not sufficiently focused on the core of the paper. We proposed a revised version that has been shortened. We tried to better highlight the novel aspects of the methodology in the revised version (L1-19).

Moreover, a similar comment applies to the introduction, which describes general properties of MPS, but does not properly introduce the specific methodological question which is faced with this work. The description given at lines 70 to 75 is not very exciting and informative. In my opinion, most of the material in section "3.1 Overview" should be anticipated in the introduction, in order to give a better presentation of the innovative character of this work at the very beginning of the paper.

Similar to the abstract, we proposed to reconsider the text in the introduction as suggested by the reviewer to provide a clearer outline of the approach. We tried to emphasize more clearly on the novel aspects of the approach. As suggested we also added some more information about the motivation of the approach and an small overview of the workflow in the introduction (L102-115). However, we decided to keep the Overview sub-section (L202-230) as we think it reintroduces the main steps of the workflow and helps the reader to wrap his/her mind around the different steps and the different elements composing the final model. The Overview sub-section has been re-write in order to be more clear.

For a long part of the manuscript, it was not clear to me whether the TIs were horizontal maps or vertical cross-sections.

We understand the possible confusion and explicitly defined that the TIs are horizontal maps view in the new version of the manuscript (L9, L109, L206, Fig. 2).

Moreover, the way in which 2D horizontal maps are used along the vertical direction should be better analysed. For instance, it would be useful to draw some vertical cross-sections in order to show the effects of the two simulation sets (with and without vertical sampling).

We agree with the reviewer and proposed to introduce a new figure displaying cross-sections of simulations with and without the sampling approach in order to effectively visualize the effects of the sampling strategy. The new figure 11 is commented in the text lines 437-441.

In fact the analysis shown in figure 10 is not clear enough.

We propose to added some information on the dissimilarity index (L428-436) in the revised version of the manuscript.

Section "3.2 Hard data set" could be improved. (a) There is some confusion between electrofacies and sedimentary facies.

We understand the confusion between the two terms. We proposed to modify the paper in order to use only the term sedimentary facies, which is more appropriate.

(b) And what about hydrofacies, which are ultimately the most important for hydraulic conductivity?

The reviewer raises an interesting remark. The main answer to this question is that two sedimentological units may have similar hydraulic conductivities but very different geometrical shapes. If we associate them to the same hydrofacies during the geostatistical simulation procedure, experience shows that the geometrical shapes of the two sedimentological units gets mixed and loses

consistency. This is why, it is often better to model first the sedimentological units and then fill them with hydraulic properties.

In addition, this process allows to account better for the hard data descriptions and the indirect geological knowledge and sedimental history of the area.

(c) What about lithological logs? Usually they are available if a borehole is drilled for geophysical logs.

The lithological logs are indeed available and used for the sedimentary facies description. We proposed to clarify this point in section 3.2 (L231-242).

(d) Details about the data set, e.g., position and borehole depth, are missing.

The position of the boreholes was indeed missing. This has been corrected and included in figure 1. We also proposed to add some information in the text regarding the borehole data, section 3.2 (L232-236).

Section "3.3 Training images" is not very convincing. It shows that different TIs give different results and some of these are not appropriate with the geological structure of the study area. This is well known and was clearly proved by some of the authors in previous papers. It is well known that the TI should mimic the structures which are expected in the study area and this should be known a priori from geological studies.

The reviewer is correct in stating that the comparison of several TIs is not novel and should be a rather standard step in any MPS simulation study. We do not claim that this is new. But we think that it is important to discuss that aspect in the framework of non stationary TI and simulations. The simulated patterns are often difficult to predict from the TI alone. Previous publications show that complex simulations can be obtained with very simple training images if proper parametrizations and trends are provided. The simulations will be very different from the TI and therefore the selection of the TI requires some trial and error testing.

Therefore, we would like to keep that part which is important for the whole procedure in our opinion. This is a step in which several conceptual models can be tested. A point also mentioned by the reviewer and we agree with him on that. Testing various TI is a step of the workflow. We think that at least to illustrate these ideas, this part of the paper can be useful for some readers and should be kept.

We proposed a slightly modified version of this section in the revised manuscript lines 247-276.

Moreover, further details should be given for figure 2a, which shows a strange sedimentary structure (see specific comment# 14).

As presented in the last comment, all of the three TIs described an alluvial system represented with the same main spatial pattern evolution. The different shapes express within a facies through the three TIs are proposed in order to test and represent at different scales different sedimentological hypotheses (eg: whether the braided river deposit cut or not the alluvial fan facies).

The facies name must not be taken in a narrow sense as they represent more a location of the depositional environment within the whole alluvial system than a facies description.

I am afraid that the term "braided river facies" is probably used in a non rigorous way. In fact, figure 2b shows the typical structure of a "braided river", with a great number of intersecting channels.

We disagree with the reviewer but we did not explain clearly enough the reasoning behind this figure. As explained in the previous answer, it is important to consider different pattern configurations in different training images and check how this will be transferred to the regional simulations when combined with non stationarity parameters and trends. This idea led to the creation of three TIs and three different representations of the braided river facies. In the first TI, the braided river facies represents the entire braided channel belt without describing its internal heterogeneity. In the second and third TI, some internal heterogeneity is included in the concept.

The reason why the entire braided river channel belt can be considered as one single channel is that it happens that there is little potential to preserve low permeability sediments in the braided river channel belt. There is internal heterogeneity in the braided system for sure at a meter scale. But at the reservoir scale, one may consider that the important contrast is the one between the braided river belt and the floodplain. Therefore, it could be reasonable to model the system in that manner.

We proposed a modified version of this in the revised manuscript lines 247-276.

In other words, areas characterised by meandering rivers show a very strong heterogeneity at relatively fine-scale. This is not properly represented by the TIs.

The same explanation stands for the meandering river, where we decided after detailed discussions with the geologists to represent the meandering river belt and not each individual meanders. This approach is explained in the figure 2 e) and is described in detail in the PhD thesis of *Issautier, Benoît. (2011). Impact des hétérogénéités sédimentaires sur le stockage géologique du CO2. University of Aix-Marseille, France : https://www.theses.fr/2011AIX10136*.

Figure 8 shows that high probability for "floodplain" facies determines approximately linear structures. It seems that these structures separate the similar geometrical features observed for "braided river" and "meandering river" facies. Is this right? This seems to be implicitly stated also in the text.

The geological concept and training images imply indeed an alternation of channels (either meandering or braided) and flood plain. When a hard data indicates the presence of one of the facies, it will impose a high probability of occurrence for this facies at the hard data location, but also upstream and downstream since the channel belts have this rather linear structure. The shape will not be exactly linear because tolerance is used for the rotation of the channel belts in the plain and the distance between the channels is not constant in the training image. Once a facies is placed, the geological consistency implies that at some lateral distance the other facies (flood plain or channel belt) will have to be present. Therefore, the general pattern identified by the reviewer is correct but the situation is slightly more complex than simple linear trends.

We updated the text to make the point as clear as possible in the paper lines 398-405.

In individual simulations, “floodplain” facies should be more widely distributed, shouldn’t it? Why these maps show a different structure? Is this due to the constraint given by the elongated features for highest probability of “river” facies?

In the individual simulations (for example Fig 7), the flood plain is rather widely distributed. The spacing observed between the river belt in the simulation output (figure 7) corresponds to the indications provided by the geologists on the site. In addition, the overall proportion of flood plain is clearly larger than the channels on every single realization. This is visible in figure 7. In the ensemble of simulations and on the probability maps (figure 8) the flood plain facies has the highest probability of occurrence as compared to the other facies. Therefore, we do not think that the flood plain facies should be more widely distributed.

The orientation is missing in all the figures and the scale length is missing in almost all the figures.

Yes we agree. The figures have been modified in order to add scale length and orientation in the revised version of the manuscript.

Technical comments :

Line 28. The acronym “PC” is used for the Continental Pliocene aquifer. Moreover, in a couple of sentences, I was confused and I read PC as “personal computer”. I understand that “PC” is probably the correct acronym based on initials of French words, but I think that “CP” would be more appropriate as an acronym for the English name.

We understand the possible confusion for the reader. We decided to not use acronyms in the revised version of the paper when describing the different geological layers and propose to use the term “Pliocene” when referring to the “Continental Pliocene layer”. We introduced the terminology at the end of the Geology subsection 2.1 (L144-145).

Line 40. Correct “1974)”. / Line 58. Correct “Hu, 2008)”. / Line 68. Substitute “,” with “.”./ Lines 95 to 97. I recommend the authors to carefully follow the international recommendations on the use of SI units and style conventions / Lines 95, 97, 110. Substitute “extend” with “extent” or “extension”. / Lines 99, 199, 213, 215, 217, 223-225, 286, 344, 345, 361, 362, 404, 419. I think the use of “meander” as adjective is not correct. I suggest to substitute “meander river” with “meandering river”. / Line 104. Substitute “plain itself” with “floodplain”. / Line 117. Substitute “of” with “by”.

These technicals comments have been corrected in the revised version of the manuscript.

Line 112. Substitute “in” with “at” before “some locations”. Rephrase “up to 8m higher on average”.

We proposed to change the sentence to : “In the 1960s, the piezometric level was on average 8 m higher as compared to the 2012 data and even artesian at some locations.” (L151-155).

Line 166. It is not clear if the TI is a map in the horizontal plane or a vertical cross-section.

As address above in the specific comments section, we explicitly defined that the TIs are horizontal maps view in the new version of the manuscript (L9, L109, L206, Fig. 2).

Line 171. Which is the direction of the x coordinate axis?

The TI is not spatially oriented, however, the x-direction can be assimilated to the east-west direction on the grid.

Lines 196-197. Clarify the expression "By studying the evolution of these response curves".

This has been clarified in the new version lines 236-241.

Line 212. The expression "an analogue river system from northern Italy" does not provide a useful information. Which river? Which kind of geological setting? Moreover, from figure 2a, the braided river facies cover an extended area and does not properly represent the internal heterogeneity of a braided river system.

We agree with the reviewer that the expression "an analogue river system" can be misleading and lack precision. We used satellite images of the Tagliamento river, which is located in Northern Italy near the town of Udine and close to the Slovenia border to create the first TI. We changed the description (L253-257) in the new version of the article

As for the comment on the "braided river facies", this point is already answered above within the specific comment 4.

Line 216. Substitute "meander objects" with "meanders". / Line 319. Substitute "doesn't" with "does not". / Line 340. Substitute "are" with "is".

This is corrected in the revised version of the manuscript.

Lines 285-286. Why "the best way to control the vertical continuity was to sample only from three facies"? Can you comment on this and explain this result?

Since the "floodplain facies" is the most frequent, sampling the facies at random location leads to an over-representation of the flood plain and tends to bias the MPS simulations. After some tests, it appeared that the easiest way to control the connectivity of the objects of interest was to sample only those facies (alluvial fan, braided and meandering river). We also decided to not sample the levee and crevasse splay facies in order to avoid constraining the whole structure of the fluvial objects too heavily.

We added these explanations in the revised version of the manuscript lines 331-336.

Line 385. Add “a” before “complex”.

We agree and replaced the sentence in the revised manuscript lines 446-447.

Lines 401 to 403. This remark is not so evident from the analysis of the results.

We proposed to clarify the explanations for figure 10 in section 4.4 (L420-428). Moreover, the new figure 11 presents cross-sections through the simulation with and without the sampling approach. We believe that this figure clarifies the effect of the sampling approach on the vertical connectivity of the river beds.

Line 495. Erase “Tectonophysics”. / Figure 3. Substitute “c)” with “b)”.

We agree and corrected it in the new version.

Answer to Referee #2 :

Specific comments :

The starting point for the proposed strategy, as stated in the abstract, is a conceptual model. The conceptual model is considered to be known deterministically. There is no mention of alternative, conceptual models. This is not trivial, and the authors need to justify this approach and suggest how to relax the constraint imposed by using a single conceptual model (see abstract lines 3-5).

We thank the reviewer for pointing out this issue in the abstract. We revised it to mention the possibility of using several alternative training images and conceptual models (L4-5).

Later, in the paper, we already considered three alternative training images (see figure 2), illustrating exactly this point. More conceptual models can be easily included in the workflow and tested.

The strategy presented here is smart in that it assimilates concepts from geology with geostatistical concepts. For example, the use of a physical-mathematical model for establishing the spatial evolution of sedimentary patterns. But some additional work is needed.

We thank the reviewer for his positive comment. Just to be sure to be well understood. The physical model that we solve is used only to get the main trends and obtain plausible patterns. We do not solve the complete coupled system of equations describing the whole processes of sediment transport, deposition, compaction, diagenesis, etc. Our approach is very much simplified as compared to proper sedimentary basin modeling approaches.

I recall some work done along this line (Item 2 above) by Steve Gorelick’s group. As I recall, it requires using weather patterns over geological time scales, for boundary conditions. So, different patterns would have a strong effect on the patterns mentioned in (2).

As we indicate above, we do not model all the processes. We just compute a trend map to control the

position of the different types of sedimentary structures in the basin. And then we rely on the multiple-point statistics approach to generate the set of realizations. This is much faster than solving the physical problem and it does not require to provide detailed initial and boundary conditions. Our approach is much simpler but it allows us to generate easily a set of realizations and get some ideas about the uncertainty while the approach based on solving the physics is much more computationally demanding. In addition, the process-based approach is not able to ensure that all the borehole data are honored. Therefore the two methods are very different and complementary.

I am trying to figure out how climate/weather conditions permeated into the modeling of sedimentary patterns. There is a brief and incomplete description of the solution of the diffusivity equation. Just a couple of lines, between Line 170 and Line 175, on the topic. The authors need to shed more light on this aspect of their approach, and to show how the math/physical model used in support of (2) is actually constructed.

As explained above, we do not account for these aspects since we want to model the system in a reasonable manner while remaining as simple as possible.

Line 65: Listing the advantages of the 2010 simulation model, the authors state "...no probability is computed...". Question is: why is that an advantage? What are the positive and negative implications or avoiding probabilistic models?

It is true that we do not explain this aspect in detail in the paper for the sake of brevity.

As explained in detail in the original paper from 2010, the direct sampling technique is a multiple-point statistics (MPS) algorithm that resamples some patterns from the training image in a stochastic manner without computing probabilities. Other MPS algorithms need to estimate the probabilities of the different patterns to produce simulations. Often, this is a problem because to estimate a probability one has to count all possible configurations and check the ones that are compatible with the data. The number of configurations can become extremely large and counting all these different configurations can become a technical limitation in terms of computing time or memory usage. Here, with the direct sampling, we resample some patterns in a manner that we ensure that the probabilities are honored but we do not compute them explicitly. This allows us to consider much more complex situations (more sedimentary facies, for example, a larger size of the patterns, or multivariate patterns) than more traditional MPS algorithms such as SNESIM. All the tests that we have done since 2010 show that this feature is an important advantage as compared to the other MPS methods because it offers much more flexibility. One possible limitation is that the time required to generate a simulation can be larger if the code is not optimized and parallelized. But this is not the case for DeeSse.

To avoid entering into a long discussion, we have added some additional references describing some features of the DeeSse algorithm lines 66-70.

In Sections 4.2 and 4.3 there is a reference to probabilistic models. Confusing, and some clarification is required.

We are sorry that this was confusing. It's true that we do not compute probabilities during the simulation step. But the models are probabilistic. Not computing the probabilities is a technical trick. It does not mean that there is no underlying stochastic process and probabilities. To try to clarify, in

addition to the new references that are provided, we added a sentence explaining that DeeSse is used to generate an ensemble of realizations from which one can estimate any relevant probabilities for the problem of interest (L68-69).

At the top of Section 4.2, the authors state as follows: "Simulating a large number of realizations enables us to calculate probability maps". That is obviously true: when you generate multiple realizations, you can compute probabilities. Question is: what is the connection between these probabilities, on one hand, and uncertainty and risk, on the other? The authors need to make a convincing case that they model uncertainty accurately. Without it, they can only say that they can generate images.

This is a very interesting and important point that has led to heated discussions in the past and that will continue for sure to raise many discussions. The debate goes much beyond the context of this paper. The question of the reviewer revisits the debate about the subjectivist and frequentist interpretations of the notion of probability. This debate has involved mathematicians, philosophers, statisticians, etc. We do not think that it is reasonable to open this debate here since we will not be able to close it for sure.

In short, we consider that we are computing a probability that we interpret as subjectivist. It is a representation of our confidence in the model that we built and the amount of information that we have. We do not claim more than that.

We think that the quality of the uncertainty estimation could be partly tested using cross-validation. This work is not presented in that paper, because our data set is too small and almost all of the models perform equally well (or bad) when there is little data available. If more data would be available, we could certainly compare the local accuracy and the calibration of the predictions of various stochastic models. We plan to do that in the future, but do not have the data for conducting that study yet. This is investigated in the paper currently submitted Juda P. : "*Juda, P., Renard, P., & Straubhaar, J. (2020). A framework for the cross-validation of categorical geostatistical simulations*". We added this reference and this explication lines 481-483.

We still want to add a word of caution, local accuracy and calibration (meaning that we predict correctly the uncertainty on the facies at a certain location) do not necessarily mean that the connectivity of the sedimentary features is well honored and that the groundwater response of the model represents correctly the true one. Therefore, even if we use cross-validation and if performances are good, it may very well happen that the groundwater predictions are not.

To summarize, we agree with the reviewer that the meaning of the estimated probability is an important issue that is not yet fully solved, but we tend to disagree with his last comment since we believe that such methods are useful to bring geological concepts in uncertainty estimations.

We need to see how the innovation (generating sedimentary patterns using a math/physical model) proposed in this study could make a difference. How would the generated images look like without the innovation? How does this innovation help in reducing uncertainty and improving accuracy? Some sort of cross-validation study (comparing results obtained with and without the improvement) could be helpful.

The author raises again an interesting point, however, we do not think that the aim of this paper is to compare the MPS approach against other ones. Other publications have already compared MPS

against SGS or pluri-Gaussian simulations and have shown the benefits of the multiple-point approach and its ability for simulating complex and realistic patterns.

The aim of this work is to present a new workflow that allows to generate complex non-stationary structures at a reservoir scale using MPS when little hard data are available. We propose to modify the introduction to better explain that objective (L102-115).

One of the novel ingredients of the proposed workflow is the computation of the trend using the solution of a diffusivity equation. We proposed to extend the discussion about the advantage of this part of the method in the conclusion (L453-456).

Regarding the advantage of using a trend map created from a math/physical model, we do not think that it would be useful to compare this approach against simulations that do not use a trend map. Indeed, it is well known from previous publications (eg. Chugunova and Hu, 2008) that using a non-stationary training image without accounting for the trend creates some disordered patterns.

Finally, as mentioned above and in the article, the cross-validation is an interesting aspect. But the lack of hard conditioning data makes its application difficult. It is planned in future work to acquire more data and to use cross validation to compare the performance of several geostatistical approaches. For the moment, we still believe that introducing the proposed workflow is interesting because it could be used by other researchers and adapted to their own studies.

Answer to Referee #3 :

General comments :

This manuscript presents a method for large-scale 3D MPS simulations in areas without the necessity of creating a 3D Training Image, which can be a cumbersome and tedious task. Especially, the presented method focuses on areas with few geological observations and little to no geophysical data (soft conditioning data). Overall, a well written paper, albeit with some technical errors, which can easily be corrected. I recommend the paper for publication. Moderate review.

We are thankful to the reviewer for his/her overall evaluation and its detailed comments on the paper. The specific and technical comments have helped to improve the manuscript.

Below we discuss more precisely the different issues raised by the reviewer and how we adjust the paper in consequence.

Specific comments :

Line 21-22: Explain why we want to skip this step. There are researchers who spend a large portion of their time building handheld 3D geological models and would not understand why it is an advantage to bypass the 3D TI.

This is an important point that was not sufficiently well explained in the introduction. We proposed to add a paragraph explaining why we think that this is an important aspect of the methodology lines 87-97.

Line 51-61: A good overview, perhaps also mention Image Quilting Simulation (IQSIM) (Hoffimann 2017 - Stochastic simulation by image quilting of process-based geological models) and other more recent methods if any.

We have added this reference in the revised version of the manuscript, we also added more recent advances made on the DeeSse algorithm (L49-60).

Line 68-69: Slightly elaborate "many options", so that the reader can grasp the advantages/disadvantages of DeeSse better.

We proposed to add recent publication on the code DeeSse but would prefer to no explain/list in detail all of the DeeSse options and parameters (L69-70).

Line 124-125: I think you mean two-point statistics. A variogram is not a geostatistical method, but a mathematical/statistical construct that is used in different geostatistical methods.

We agree on this point and have replaced "variogram" by "two-points statistics" in the new manuscript line 41.

Line 180-181: Making 3D Tis is not "too complex". In fact, in the literature, many studies are presented where handheld 3D geological models are created, which are essentially 3D TIs. Rephrase it to emphasize that it is a difficult, time consuming and subjective way of modeling, but NOT "too complex".

The reviewer is right on the subjective use of "too complex" and that some other studies lead to the creation of 3D geological models, which could be used as TI. We modify the manuscript in consequence line 19.

Line 201: What geological map? You should show it or cite it. If it is the one in Figure 1, then include a reference to figure 1 here.

We added the reference to the cited geological map (L243-245).

Line 204-205: If it is essential to condition the model to the geological map, then you should describe how you do this.

We agree on this point and proposed to add some information on the process lines 243-247 of the revised manuscript.

Figure 3 caption: What is c) referring to? And b) is not mentioned. Needs to be fixed. Also, the grey model makes sense, but you should still describe it in the figure caption.

It was a typo in the caption and modified the caption of the figure 3.

Figure 4: In the b) and c) it would be a lot better if you added a thin black line to mark the outline of the layers, especially in relation to the stacked trend map in c). As for the current state of the figure I

do not really get a lot of information from the stacked trend maps since all the colors of the different layers are identical by design.

The stacked trend map only shows the progradation of the trend as we move upward in the layers, the dark blue color is moving gradually towards the sea as the system evolves. A new 3D view is proposed in the revised version of the figure 4.

Line 256-257: What do the diffusivity equations look like? And what is considered "proper boundary conditions"?

To answer this comment, we rewrite the text in the trend maps section 3.5 (L298-309).

Line 274: Insert a reference to Figure 5b) here.

This has been corrected in the revised version.

Line 276-277: Since river system are highly dynamic in nature, and since the reader has no idea about the sedimentation rates over the last 6 My in the given sedimentary basin, you should probably state why we can safely assume that the variation of the paleo orientations are encompassed by +/- 10 degrees of the values observed at the surface currently.

It is true that river systems are highly dynamic and that their bed orientations can vary through time. However, since our TI encompasses the whole river bed, as shown in figure 2d, we do not expect to see strong orientation changes. The rotation map is derived from interpretation and thus cannot be taken as true fixed values of the paleo orientations. The +/- 10 degrees of tolerance is fixed to take into account this uncertainty. This tolerance also helps to not overconstrain the model and to accommodate the location of the patterns to the hard data during simulations.

We think that the sentence "The orientation map is based on interpretation and therefore uncertain. DeeSse allows to account for this uncertainty. A tolerance of +/- 10° is considered and added/subtracted to the kriged map to obtain two rotation maps..." gives enough information on the reader on the fact that the kriged value is not the true orientation of the paleo river and that some flexibility must be left to the algorithm to simulate the orientation of the patterns.

Line 285-287: Seems a bit discerning, can you elaborate as to why the vertical continuity was not as good when all 6 facies were included for sampling?

This question has already been raised by the reviewer#1. We propose to copy the answer of this comment :

Since the "floodplain facies" is the most frequent, sampling the facies at random location leads to an over-representation of the flood plain and tends to bias the MPS simulations. After some tests, it appeared that the easiest way to control the connectivity of the objects of interest was to sample only those facies (alluvial fan, braided and meandering river). We also decided to not sample the levee and crevasse splay facies in order to avoid constraining the whole structure of the fluvial objects too heavily.

Figure 7: You should always introduce each sub figure in order a) -> b) -> c), not a) -> c) -> b). Also, a very important detail is that nowhere in the paper do you present a vertical slice, or profile, of the simulated models, so the reader cannot see how bad/well the vertical constraints worked in comparison to a full 3D TI. It would be easy to add a cross section view in this figure.

The caption for figure 7 has been corrected, the b) and c) were simply swapped.

We understand the need of cross section view in order to visually inspect the effect of the vertical sampling approach on the simulation outputs. We propose a new figure 11 including these elements. The figure is presented at the end of this document. We also add a small description in section 4.4 (L437-441).

Line 346-348: How do the maps explain that the model is not over constrained? It might be obvious to you, but not necessarily the reader.

We agree with the reviewer that more information needs to be included for the reader. We proposed a revised version for the manuscript (L398-405) providing clearer explanations.

Lines 385-387: I think you are going need to touch on the strengths/weaknesses when making a comparison like that. The so-called classical MPS studies simply have a lot of geophysical/conditioning data available to them, and will, in large, be better conditioned to the actual subsurface. On the other hand, your method is clearly advantageous when you do not have a lot of geophysical/conditioning data available, but of course will not be as nicely conditioned to the actual subsurface. There are many places in the world where they need methods like this, since they do not have elaborate geophysical data sets available to them.

We think that the presented method should not be viewed in opposition to other methods where geophysical data are available. There is no strength in lacking soft information, the objects are not well described neither in their size nor their location and validation approach cannot be performed when lacking conditioning data.

The proposed workflow is only an alternative that tries to take into account most of the available conceptual knowledge.

Line 408-409: How are they satisfactorily reproduced? Based on what? Is it solely based on the boreholes being conditioned correctly and the simulations resembling the TI? Then, it would be nice to show some statistics regarding how well the boreholes and simulations agree.

The facies proportions are satisfactorily reproduced base on the fact that they are similar to the borehole facies proportion distributions, excepted for the alluvial fan proportion that is under-represented in the hard data but compensated with the influence of the TI.

We believe that this is shown in figure 10 a and explain in the sub-section 4.4.

Specific comments :

In general, it is not called a “meander river”, but a “meandering river”. This needs to be fixed.

This has been corrected in the manuscript and in the figures.

Line 28: The abbreviations for Marine Pliocene aquifer is PMS. Perhaps this is an abbreviation that makes sense in relation to the French name for the unit, but in order to make the paper more readable I recommend using MPA, which makes more sense. Line 28: Similarly, the abbreviation for Continental Pliocene is PC. It would be more fitting to use CP.

This comment was already mentioned by the reviewer#1. Here is the proposed answer :

We understand the possible confusion for the reader. We decided to not use acronyms in the revised version of the paper when describing the different geological layers and propose to use the term “Pliocene” when referring to the “Continental Pliocene layer”. We introduced the terminology at the end of the Geology subsection 2.1 (L144-145).

Line 68: Change “It” to “it”, i.e. no capital letters after comma. / Line 76-77: Add “:” after “The paper is structured as follows”, followed by changing “The” to “the”. / Line 78: Missing comma after DeeSse algorithm, and “Section 3” should not have a capital letter. / Line 95: You mean the “extent” and not “extend”. / Line 238: change “express” to “expressed”. / Line 360: Change ”the alluvial fan dominate” to “the alluvial fan dominates”.

These technicals comments have been addressed in the revised version of the manuscript.

3D Multiple-point Statistics Simulations of the Roussillon Continental Pliocene Aquifer using DeeSse

Valentin Dall'Alba[1], Philippe Renard[1], Julien Straubhaar[1], Benoit Issautier[2], Cédric Duvail[3], and Yvan Caballero[2]

[1]Center of Hydrogeology and Geothermics (CHYN), University of Neuchâtel. Rue Emilie Argand 11 CH-2000, Neuchâtel, Switzerland
[2]French Geological Survey (BRGM)
[3]GEOTER SAS, FUGRO Group

Correspondence: Valentin Dall'Alba (valentin.dallalba-arnau@unine.ch)

Abstract. This study ~~presents~~ introduces a novel workflow to model the ~~internal~~ heterogeneity of complex aquifers using the multiple-point statistics algorithm DeeSse. We illustrate the ~~applicability of this workflow on~~ approach by modeling the Continental Pliocene layer of the Roussillon's aquifer in the region of Perpignan (southern France). ~~This work is part of a project aiming at assessing the groundwater dynamics of this Mediterranean aquifer in the context of a growing population, climate change, and increasing pressure on the freshwater resources. We focus here on the geological heterogeneity of the Continental Pliocene layer because it is expected to influence possible saltwater intrusion process and its corresponding uncertainty quantification. The main aim of the paper is therefore to describe the procedure that is used to model the aquifer heterogeneity with a relatively small number of direct geological observations and a well defined geological concept.~~ When few direct observations are available, ~~the~~ statistical inference from field data is difficult if not impossible, and traditional geostatistical approaches cannot be applied ~~easily because variogram inference is difficult~~directly. On the opposite, multiple-point statistics simulations can rely on ~~a~~ one or several alternative conceptual geological model ~~. Here, the conceptual model consists not only of a training image displaying the spatial organization of the main sedimentological elements in space, but also in a set of additional information such as general trends and paleo orientations of the sedimentological features. The~~ provided using training images. But since the spatial arrangement of geological structures is often non-stationary and complex there is a need for methods allowing to describe and account for the non-stationarity in a simple but efficient manner. The main aim of this paper is therefore to propose a workflow, based on the direct sampling algorithm DeeSse~~can be used in this context to model the expected heterogeneity. The workflow involves creating 2D~~ , for these situations. The conceptual model is provided by the geologist as a two-dimensional non-stationary training ~~images~~ image (TI) ~~coupled during simulation with auxiliary information and controlled by hard conditioning data obtained from interpreted electrofacies~~in map view displaying the possible organization of the geological structures and their spatial evolution. To control the non-stationarity, a 3D trend map is obtained by solving numerically the diffusivity equation as a proxy to describe the spatial evolution of the sedimentary patterns, from the source of the sediments to the outlet of the system. A 3D continuous rotation map is estimated from ~~paleo orientations~~ inferred paleo-orientations of the fluvial system. Both trend and orientation maps are derived from geological insights gathered from outcrops and general knowledge of processes occurring in these types of sedimentary environments.

Finally, the 3D model is obtained by stacking 2D simulations following the paleo-topography of the aquifer. The vertical facies transition between ~~two~~ successive 2D simulations is controlled ~~by both the hard conditioning data set and by simulating~~ partly by the borehole data used for conditioning and by a sampling strategy. This strategy accounts for vertical probability of transitions, which are derived from the borehole observations, and works by simulating a set of conditional data points from one ~~simulation to another~~layer to the next. This process allows us to bypass the creation of a 3D training image ~~while preserving the vertical continuity of the sedimentary objects.~~ which may be cumbersome while honoring the observed vertical continuity.

1 Introduction

It has been shown, for example by Naranjo-Fernández et al. (2018), that accounting for heterogeneity is an important step in producing realistic hydrogeological models and to properly manage the water resource, especially in a context of global climatic changes. The present study proposes a new multivariate workflow, using a multiple-point statistics (MPS) approach, to model the spatial heterogeneity of complex alluvial aquifers. The workflow is applied to the Roussillon aquifer, which is a multi-layered system composed of the Marine Pliocene aquifer~~(PMS)~~, the Continental Pliocene aquifer~~(PC)~~, and the Quaternary aquifer~~(QT)~~. Located along the southernmost part of the French Mediterranean coast, near the Spanish border, this system is used intensively both for drinkable water and irrigation (Aunay et al., 2006). From its social and economic importance, understanding the aquifer is essential for the authorities to ensure a long term and sustainable management of the resource. Since one of the largest source of uncertainty is the identification of the hydraulic conductivity field, it has been decided to ~~first~~ focus on the modeling of the complex geological heterogeneity of the Continental Pliocene layer. This layer consists of alluvial deposits and presents a high level of internal heterogeneity.

To model the heterogeneity, different geostatistical methods have been developed and used in the last decades ~~(de Marsily et al., 2005)~~ (Koltermann and Gorelick, 1996; de Marsily et al., 2005). They were employed in different fields going from risk assessment, resources management, mining or petroleum engineering (Matheron, 1963; Strebelle et al., 2002; de Carvalho et al., 2017). All these methods aim to model the variables of interest at locations where they have not been measured. Traditional geostatistical methods are based on a covariance or variogram models inferred from the data. Kriging (Matheron, 1963) provides the best linear unbiased estimator, it is fast, and produces a smooth interpolation. Multi-Gaussian simulation methods, such as ~~SGS~~ Sequential Gaussian simulation approach (SGS) proposed by Journel (1974)~~)~~, are able to generate random fields, depicting the spatial variability of the variable of interest. Truncated Gaussian simulation methods (TGS or PGS) allow to generate discrete realizations where the spatial relation between the facies (categories) are derived from one or several underlying multi-Gaussian random fields (Matheron et al., 1987). However, these methods are based on two-point statistics and cannot reproduce some geological features such as the sinuosity of a channel or realistic sedimentological patterns. Hence, they are not always suitable for modelling the expected heterogeneities in geological reservoirs. Multiple-point statistics ~~(MPS) has~~ methods have been developed since the 90's to overcome these limitations. MPS techniques allow to generate random fields reproducing the spatial statistics given in a training image (TI), which is a conceptual model that integrates the geological knowledge of the area of

interest. Moreover, unlike traditional approaches, MPS does not require to define an analytical model to describe the statistical spatial distribution of the modelled variable of interest, instead it infers it in an implicit way from the TI provided by the user (Hu and Chugunova, 2008).

Many MPS algorithms have been developed over the years. The general principle consists in sequentially populating the simulation grid while reproducing the patterns (spatial statistics) present in the TI. For example, in SNESIM (Strebelle et al., 2002), the statistics of patterns on a pre-defined geometry are stored in a tree shape database that is built by scanning the whole TI before starting the simulation. Then, the simulation proceeds pixel by pixel, a value is drawn randomly according to probabilities conditioned by the surrounding patterns and computed from the data base. As a consequence, the method is memory consuming and limited to the simulation of categorical variables. In IMPALA (Straubhaar et al., 2011, 2013), the limitation due to the memory is alleviated by using a list shape database, and non-stationary TIs can also be handled with the use of auxiliary variables ~~(Chugunova and Hu (2008))~~(Chugunova and Hu, 2008). In other algorithms, such as FILTERSIM (Zhang et al., 2006)~~or CCSIM (Tahmasebi et al., 2012)~~ , CCSIM (Tahmasebi et al., 2012) or IQSIM (Hoffimann et al., 2017) , the simulation grid is filled by directly pasting or quilting patches, *i.e.* several pixels at a time. FILTERSIM ~~allows the simulation of continuous variables~~uses a set of filters to reduce the dimension of the problem, whereas CCISM is based on cross-correlation between patches. IQSIM proposes a new approach that bypasses traditional ad-hoc weighting of auxiliary variables. The main drawbacks of patch-based methods is often their difficulty to honour conditioning data.

One of the most flexible MPS algorithms is the Direct Sampling (Mariethoz et al., 2010). It is a pixel-based method, where the simulation of one pixel consists in randomly searching for a pattern in the TI that is similar to the pattern centered on the considered pixel in the simulation grid, and then copying the value of the variable from the TI. ~~Hence, it~~ It has the advantage of making database creation unnecessary, ~~no probability is computed , and~~ it does not computed probability, and can handle patterns of varying geometry~~are handled~~. By adapting the way of comparing the patterns in the TI and in the simulation grid, the algorithm is able to deal with categorical and continuous variables, as well as with the joint simulation of multiple variables. In this work, we use the direct sampling algorithm implemented in the DeeSse code (Straubhaar, 2019)~~,~~. It is parallelized and offers many options to constrain the ~~simulation~~ stochastic simulations such as continuous rotation/affinity maps or proportion targets. Finally, by generating an ensemble of realizations, it is then possible to estimate any probability of interest from the different facies maps. More details about the features of the DeeSse code are provided in Meerschman et al. (2013); Straubhaar et al. (2016, 2020).

~~But~~ The choice of a simulation technique to model an aquifer at a regional scale ~~, a very~~ depends from different factors. One important aspect is ~~to account for all the~~ the amount of data available. When the amount of data is large, it is possible to infer rather accurately the statistics describing the spatial variability from the data. Probability distributions about the different rock types, variograms, and spatial trends can be directly estimated and used in the simulation process. This situation often occurs in the mining industry, for example where very large number of drill holes are made during the exploitation of an ore deposit. The configuration is very different in other situations, such as the Roussillon plain, where only a few boreholes are available for a large study area. It becomes then difficult if not impossible to estimate accurately those statistical parameters from the data set. One has then to rely more heavily on indirect data, geological concepts and analogy with other sites. In these situations, one

could borrow statistical distributions, variograms and orders of magnitude of correlations lengths from data bases of similar environments such as those developed by Colombera et al. (2012). The issue with that approach is that the simulations may be constrained only by a few data points and therefore the final variability among the simulations will be excessively large and the geological features will not be properly represented because the field data will not compensate the lack of geological concept in a variogram based geostatistical approach. An object based method would respect better the geological knowledge because the user will have to explicitly define the shape of the objects and this approach could be an interesting solution for these situations with an important data gap. Here, we rather consider the use of MPS. As for the object based approach, it allows integrating directly geological knowledge in the stochastic simulation process.

When using MPS, an important part of the process is the construction of the training image. We first want to note that the conceptual sedimentological models are usually represented in 2D map views or block diagrams and geologists are used to express their understanding of a system by drawing such maps and cross sections. Furthermore remote sensing data or geological maps are widely available and can be used to refine these 2D conceptual models. Accessing 2D training images is therefore easy and simple. However, the standard MPS workflow requires a 3D training image to generate 3D simulations. Getting the 3D training image from 2D concepts is not a simple task. It may require a significant amount of tedious work to construct manually a 3D training image from the 2D concepts. Therefore, previous research was devoted to the design of MPS algorithms able to use 2D training images directly as input for 3D simulations (Comunian et al., 2012; Cordua et al., 2016). Here, we propose a simple approach that allows the user to avoid the step of the 3D training image construction. This is not mandatory. If a 3D training image is available, it can easily be used in the workflow, but if it is not available it should not be a limitation as we will illustrate in the paper.

Another very important aspect to take into account at the regional scale are the statistical non-stationarities ~~due to the geological process~~ resulting from geological processes such as the location of the sources of the sediments, their transport, deposition, and so on. The application of MPS to a real case ~~, requires~~ requires therefore more than just an efficient MPS code and a good training image. It ~~requires also~~ also requires to develop a methodology and a workflow to account for all those aspects.

The aim of this paper is therefore to introduce ~~such~~ a global workflow allowing to incorporate most of the available geological knowledge into a plausible heterogeneity model and to illustrate the method on the Roussillon plain. ~~The workflow~~ This approach is generic and can be applied to any other case where the available data are scarce compared to the geological knowledge. The ~~paper is structured as follows. The~~ workflow includes a series of steps that are described in detail in the paper. Based on the borehole and geological knowledge of the site, a plan view non-stationary training image displaying the main sedimentological features is designed. In this paper, we limit ourselves to the construction of a 2D training image since there are many situations in which the cross sectional view at the scale of the aquifer is much less well known than the expected spatial organization of the sedimentary layers on a 2D horizontal plane. The vertical transitions are controlled using probability of transitions derived from the boreholes. To control the lateral transitions and non stationarity, a 3D auxiliary map representing a proxy of the evolution of the system from the source of the sediment to the output is modeled by solving a diffusivity equation. The boundary conditions imposed to the diffusivity equation allow to account for the paleo-input zones and the lateral geometry

of the aquifer. In addition, the proposed workflow accounts for the paleo orientations of the sedimentary system and its related uncertainty as inferred from field observations. This work shows that such an approach can be efficient to simulate realistic alluvial systems matching the conceptual knowledge of the system.

The paper is structured as follows : section 2 introduces ~~some~~ the background information regarding the geology and hydrogeology of the Roussillon aquifer, ~~followed by additional information on~~ and the DeeSse algorithm~~. Section~~ , section 3 describes the workflow, and ~~the last section~~ section 4 presents the results. The paper ends with a discussion and conclusion.

2 Background information

2.1 Geology

Located in southern France, this ~~700~~800 km^2 sedimentary basin is limited by the foothills of the Pyrenees to the south and west, the Corbières massif to the north and the Mediterranean Sea to the east (Fig. 1). This basin originates from the opening of the Gulf of Lion (Oligocene to Miocene) before being largely eroded by the Messinian Salinity Crisis (MSC) (Clauzon et al., 2015). It is with the drying up of the Mediterranean Sea that the Miocene was exposed and eroded, approximately 6 My ago (Lofi et al., 2005). During the Pliocene, the basin was filled up again, with Gilbert delta reworking the sediments generated by the sub-aerial Messinian unconformity. The sediments grade to wave-dominated deltas (Sandy Marine Pliocene~~or PMS~~) to fluvial dominated delta with the continental part corresponding to the Continental Pliocene~~(PC)~~. On top of the stratigraphic pile, Quaternary sediments associated with rivers and lagoon systems have been deposited.

The Pliocene layer is composed of different sandstone units separated by silt and clay layers of low permeability (Duvail, 2012; Aunay et al., 2006). The main source of sediments came from the weathering of the massifs surrounding the Roussillon's plain. Its depth increases towards the coastline, where its maximum thickness reaches 300 ~~m~~ m (Duvail et al., 2005).

Based on field observations, the ~~PC~~ Continental Pliocene can be considered as a classical fluvial sedimentary system. Near the relief, the association of high energy systems and the large amount of available sediments created alluvial fan deposits, composed of sandstone conglomerates. These alluvial fans have an ~~extend~~ extent of 1-3 km radius and can be more than 10 m thick. Fans merge together producing larger bodies of 3 to 6 km wide and over 60 m thick. The alluvial fans rapidly evolve to braided river deposits composed of coarse sands and sandstone conglomerates. These braided structures have generally an ~~extend~~ extent of 100-150 m width and are 1-5 m thick. It appears that these networks can be laterally and vertically well connected, forming very dense and wide objects near their sources. With the decrease of the sedimentary slope, the structures tend to evolve ~~to meander rivers~~toward meandering river structures. Their deposits are still relatively coarse, yet much more sorted, and well contained within a single channel, their width reaches up to 300 m and their thickness up to 12 m. The connectivity of the river bed deposits is hard to observe either in the vertical or in the horizontal directions. Three other sedimentary elements are also intrinsically developed within the alluvial plain. The first two are the crevasse splay deposits and the levees, which are both directly related to the river's banks flooding dynamic. The last element is the ~~plain itself~~ floodplain characterized by a fine grained (silt to shale) sedimentation corresponding to the decanting process of flooding events. In the

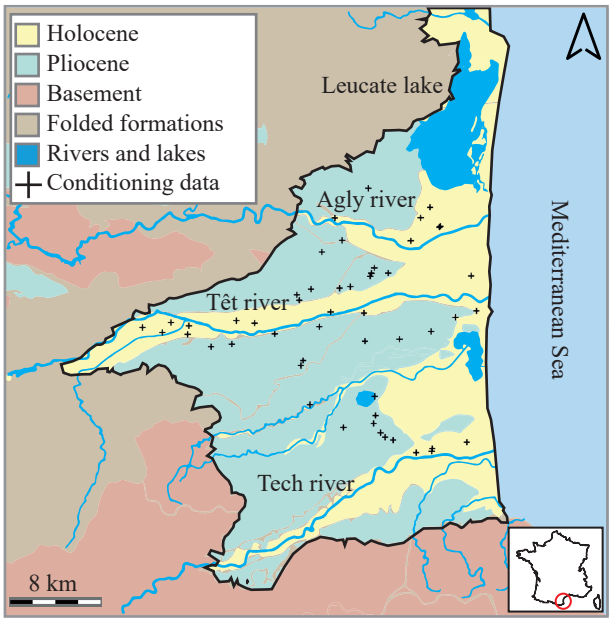

Figure 1. Simplified geological map of the Roussillon Plio-Quaternary aquifer.

following, and because we do not consider the deeper Marine Pliocene formations in this paper, we refer to the Continental Pliocene layer/aquifer as Pliocene layer/aquifer.

2.2 Hydrogeology

From a hydrogeological perspective, the study area contains two main aquifers; the Quaternary located in the shallow alluvial deposits along the rivers (Agly, Têt and Tech), and the Continental and Marine Pliocene aquifer located deeper and covering the whole basin (Fig. 1). These aquifers are exploited for agriculture and domestic use.

Due to its large ~~extend~~extension, both onshore and offshore, the Pliocene's aquifer represents a large water reservoir. However, due to uncertainties related to its properties and recharge processes, the management of this resource is difficult. In the 1960s, the piezometric level ~~in the PC was artesian in some locations and up to~~ was on average 8 m higher ~~on average~~ as compared to the 2012 data and even artesian at some locations. In recent years and close to the seashore, this exploitation has lowered the groundwater level below sea level during the summer months, when withdrawals are most intense. This situation raises concerns about seawater intrusion risk on the coastal part of the Pliocene aquifer.

As a consequence of climate change, groundwater reserves and recharge may decrease in the near future. For a scenario where the average annual temperature increases ~~of~~ by 1.5 C°associated with a decrease in precipitation rate, rivers flow could drop by 40 % over the next 30 years (Chauveau et al., 2013), which will automatically create new stress on the groundwater resource. Considering that the multi-layer Plio-Quaternary Roussillon's aquifer accounts for almost 80 % of the resources used

for drinking waters, there is an urgent need to understand its behavior in order to manage this resource in a sustainable manner to face global change impacts (Caballero and Ladouche, 2015).

2.3 Multiple-point statistics and DeeSse

The essential ingredient of MPS techniques is the TI. The TI is a conceptual model displaying the structures the user wants to simulate. The use of TI gives flexibility and creativity to the modeller. Unlike some other geostatistical methods such as ~~variogram~~two-point statistics, utilization of training image allows specialists from different fields to discuss together about the geometry and the type of heterogeneity of a model.

A TI can either be stationary or non-stationary. Stationary TIs are easier to use, they display a repetition of patterns with a homogeneous spatial distribution, *i.e.* the same type of spatial features is present everywhere in the grid. On the opposite, non-stationary TIs, displaying different kinds of structures depending on the location, they generally include more information and are more complex. When working with non-stationary TI, some rules must be observed in order to produce realistic simulations. Since the repetition of patterns is not homogeneous on such TI, one or several auxiliary variables are required to describe patterns spatial distribution. In the simulation grid, corresponding auxiliary variables are defined to control the spatial location of the structures that have to be simulated (Chugunova and Hu, 2008). With this information, patterns are not mixed together when simulated and trend characteristics can be reproduced. Auxiliary ~~variable~~ variables for the simulation grid are often called trend maps, because they allow to control the ~~trend~~ trends of the simulated structures.

A rotation map can also be used to orientate differently the patterns in the simulation grid compared to their orientation in the TI. Hence, the specific spatial features displayed in the TI can follow the same orientation everywhere, which facilitates the construction of the conceptual model, whereas the rotation map ~~is used to define~~ defines the local orientation in the simulation grid. Such map consists of angle values defined on the simulation grid ~~: at~~ for each pixel, the given angle ~~specifies~~ specifying a rotation that must be applied to the TI structures.

~~The~~ As previously mentioned, the DeeSse code is used in this project, which is an implementation of the direct sampling method (Mariethoz et al., 2010). The algorithm is controlled by three main parameters, e.g. n- number of neighboring nodes, f ~~- scan~~ - scan fraction, t ~~- distance~~ - distance threshold. The first one, n, defines the maximum number of nodes considered when comparing a pattern in the TI and in the simulation grid. At the beginning of the simulation, these n closest points are likely to be located far away from the simulated point. ~~However, as~~ As the simulation progresses, the density of simulated point increases and the n closest points are ~~located near~~ starting to be located closer to the central point. This feature enables DeeSse to reproduce structures of all sizes during the simulation, starting with large ones and finishing with small and fine structures (Mariethoz et al., 2010). The second parameter is the threshold value t. When comparing patterns during the simulation, DeeSse calculates the pattern similarity between the TI and the simulation grid with a distance value. A perfect match between the patterns represents a distance of 0 and completely different patterns correspond to a distance of 1. If the distance calculated at the first random position in the TI is larger than the threshold, another point is chosen randomly in the TI and the distance is re-calculated. This is repeated until the value of the distance has reached the threshold or if a perfect match is found, then DeeSse copies the value of the central point found in the TI into the simulation grid. The last parameter ~~,~~ f, allows to limit the

simulation time while conserving realistic patterns reproduction. If a fraction f of the TI is scanned without finding a pattern satisfying the threshold condition t, then the best node scanned so far (corresponding to the minimal distance between patterns) is retrieved. The same principles are used for categorical and continuous variables with an adapted definition of the distance. For multivariate simulation, one pattern per variable is considered, with the same central node, and one threshold value per variable.

3 Materials and Methods

This section presents the different elements that constitute the proposed MPS workflow. The elements are presented in their chronological order. The section starts by an overview of the workflow before describing the different steps more in ~~details~~detail.

3.1 Overview

The first step of the workflow consists in interpreting the geophysical logs and geological field observations to establish the geological concept and build the hard conditioning data set.

The second step consists of converting these observations and concepts into one or several training images. This step is an iterative task, the modeller works with the geologist and they come up with one or several representative TI(s) of the system.

~~Here~~In the Roussillon case, the TI used for the ~~PC layer~~Pliocene, is a 2D non-stationary ~~TI~~ conceptual plan view of an alluvial system composed of 6 sedimentary facies. The TI imposes constraints regarding the geometry of the simulation grid and on the auxiliary information that have to be incorporated in the model. ~~Regarding the PC layer, the~~

The third step is the creation of a suitable simulation grid and its associated auxiliary variables. The Roussillon' simulation grid is created based on the bottom topography of the ~~PC~~Pliocene, in a flattened space, where 2D simulations can be generated in layers sharing the same age of deposition.

In order to cope with the non-stationary TI, we use two auxiliary variable maps, one for the TI and one for the simulation grid. For the TI, the auxiliary variable is simply the x coordinate that is re-scaled between 0 and 1, this variable will inform the algorithm on the patterns location in the TI. For the simulation grid, we compute the auxiliary variable by solving numerically a diffusivity equation with proper boundary conditions allowing to mimic the general trend of sediment transport from the sediment source, on the west of the basin, to the coast. The last ~~element~~ auxiliary information that is incorporated in the model is rotation maps. The use of the direct sampling algorithm allows us to work with continuous rotation maps, defined ~~through~~ for all the nodes of the grid (Mariethoz et al., 2010), whereas classic MPS techniques require to define rotation zones of unique value (de Carvalho et al., 2017). In addition, two continuous rotation maps are used to define the rotation bounds for the simulation with a tolerance of ~~±~~+/- 10° on the rotation values. Theses rotation maps are obtained by kriging data that constrain the paleo-orientations of the main paleo-rivers.

The 3D model is then composed of stacked 2D simulations constrained by 3D auxiliary information. ~~It appears that the creation~~ As discussed in the introduction, this approach allows avoiding the construction of a 3D TI ~~would have been too complex in regard of the available knowledge of the facies that compose the plain~~that could be cumbersome. To compensate

for this choice and to take most of the information ~~of~~ available from the hard data set, the 3D grid is created with a rather fine resolution along the z axis (~~2m~~2 m), which corresponds to the smallest body's dimension encountered in the plain. The vertical transition between facies is controlled by simulating additional conditioning data points between two 2D simulations. The values assigned to these sampled points are based on the vertical transition distribution of the facies, inferred from the hard data set. This process allows to bypass the creation of a 3D TI and to simulate in 2D ~~with objects of~~ simulation, 3D objects with a realistic z dimension.

The last step consists in generating a set of simulations to characterize the uncertainties. Probability and entropy maps are computed to summarize this information.

3.2 Hard data set

Hard data correspond to field observations assigned to cell values in the simulation grid. The hard conditioning data set of the ~~PC~~ Pliocene model is composed of 52 well logs (lithological, gamma-ray and resistivity logs), which have been described and interpreted in term of ~~electrofacies~~sedimentary facies. The boreholes are not homogeneously distributed on the plain ~~,~~but are mainly located along the Têt river and in the central zone of the Roussillon's plain (Fig. 1). Their depths range from 20 m to 150 m and they are on average 77 m deep.

The gamma ray and resistivity logs allowed to identify changes in sedimentary deposits and grain distribution along depth. Sand sediments have a small gamma ray response producing small peaks on the curve, whereas clay sediments produce high response peaks due to their high content in radioactive elements (Serra O. et al., 1975). By ~~studying the evolution of these response curves, the sedimentary facies can be identified and assigned~~ analyzing the gamma-ray and resistivity responses at a certain depth coupling with their vertical evolution, it is possible to identify and assigned a sedimentary facies at a certain depth range. A complete description of the interpretation process ~~for the electrofacies of the PC layer~~ of these facies can be found in Duvail (2008).

~~As presented in the geology section 2.1, six facies are identified in the outcrops; alluvial fan, braided river, meander river, crevasse splay, levee and floodplain deposits. Due to the small size of the levee deposit, its identification on the logs is not possible and would lead to misinterpretations. Therefore, only 5 out of the 6 facies are interpreted in the well logs.~~

The hard conditioning data set also incorporates geological information from the geological map of the Roussillon (Genna, 2009) . These data correspond to the mapped ~~PC alluvial fan outcrop and are associated to the alluvial fan facies. It is essential to condition the model to~~ Pliocene alluvial fan outcrops. We transformed the polygons from the geological map ~~where the simulated layers are exposed~~into conditioning data set for the simulation. The facies assigned to these outcrops corresponds to the alluvial fan facies.

The final conditioning set results of ~~3500~~ 3'500 interpreted points, that are being used during the simulation as hard conditioning data.

3.3 Training Images

Based on field observations, well logs analysis and the general understanding of the sedimentary processes composing the PCPliocene, three TIs, corresponding to different possible conceptual representations of the PCPliocene, are created and tested in 2D simulations (Fig. 2). As discussed by Høyer et al. (2017), the creation of the TI is an iterative task and it is always preferable to compare TIs not only on their structural aspects but also on the MPS simulation outputs.

The first TI (Fig. 2a) is created based on a conceptual interpretation of an analogue riversystem from northern Italy where levees are not representedvisual interpretation of satellite images of the Tagliamento river, which is located in Northern Italy near the town of Udine close to the Slovenia border. The entire channel belt is considered as the deposition zone. This first TI neither represents the small scale internal structures of the river deposits nor the levee structures. The output of the 2D MPS simulation using this first TI resulted TI results in the creation of a too large number of small braided/meander meandering river deposits on the plain. Moreover, the alluvial fan facies is not simulated correctly, cutting heavily through braided river in the north-west part of the plain. The second TI (Fig. 2b) is created based on a more conventional conceptual representation of braided/meander meandering river system. It presents more complex braided structures and larger meander objectsmeandering river beds. The simulation output is composed of wider meander meandering river deposits compare to what is observed in the outcrops. Moreover, the alluvial fan deposits -dark blue facies- are under-simulated compared to the observed alluvial fan deposits. Finally, we construct a third conceptual model of TI (Fig. 2c), which was constructed is produced by trial and error adjustments. This TI is composed of six sedimentary facies (Fig. 2b) and displays the evolution of an alluvial system from the mountain (sediment source) to the seashore, without including the estuary part (Nichols and Fisher, 2007)(Fig. 2d). In this last TI, meander meandering river channels have a straight shape due to the fact that this training image is not a snapshot of a fluvial system but rather an integrated view of a sedimentary system through time. This concept is illustrated in Fig. 2e, with the meander meandering river facies used as an example. At $t = 0$, the meander meandering river bed follows one path, controlled by the sedimentary slope and the topography. At $t = 1$ the meander river this bed would have laterally migrated, which could cut through the previous one. Finally, at $t = 2$ it is possible to define an area of high river bed occurrences, where all the meander meandering river bed facies would be located. The last one, ~~$t = 3$~~$t = 3$, highlights the only possible location where crevasse splay and levee can be preserved, on the borders of the river bed. It is this TI that is used for the next modelling part of the workflow.

The final TI is composed of 100×125 cells with a 100×100 ~~m~~ m dimension. These dimensions are chosen in order to avoid any affinity transformation during the simulation. To propose some variability and not over control the transition distance between braided and meander meandering river deposits, the final TI laterally reproduces different fluvial systems (Fig. 2c). The dimension of the crevasse splay deposit increases with the decrease of the sedimentary slope (assuming the sedimentary slope decreases as we move from the sediment sources to the seashore). Finally, the levee facies is incorporated in the TI outside of the meander bed meandering river objects. Even if this facies is not described in the boreholes data, its spatial location will be constrained by the meander meandering facies during simulation.

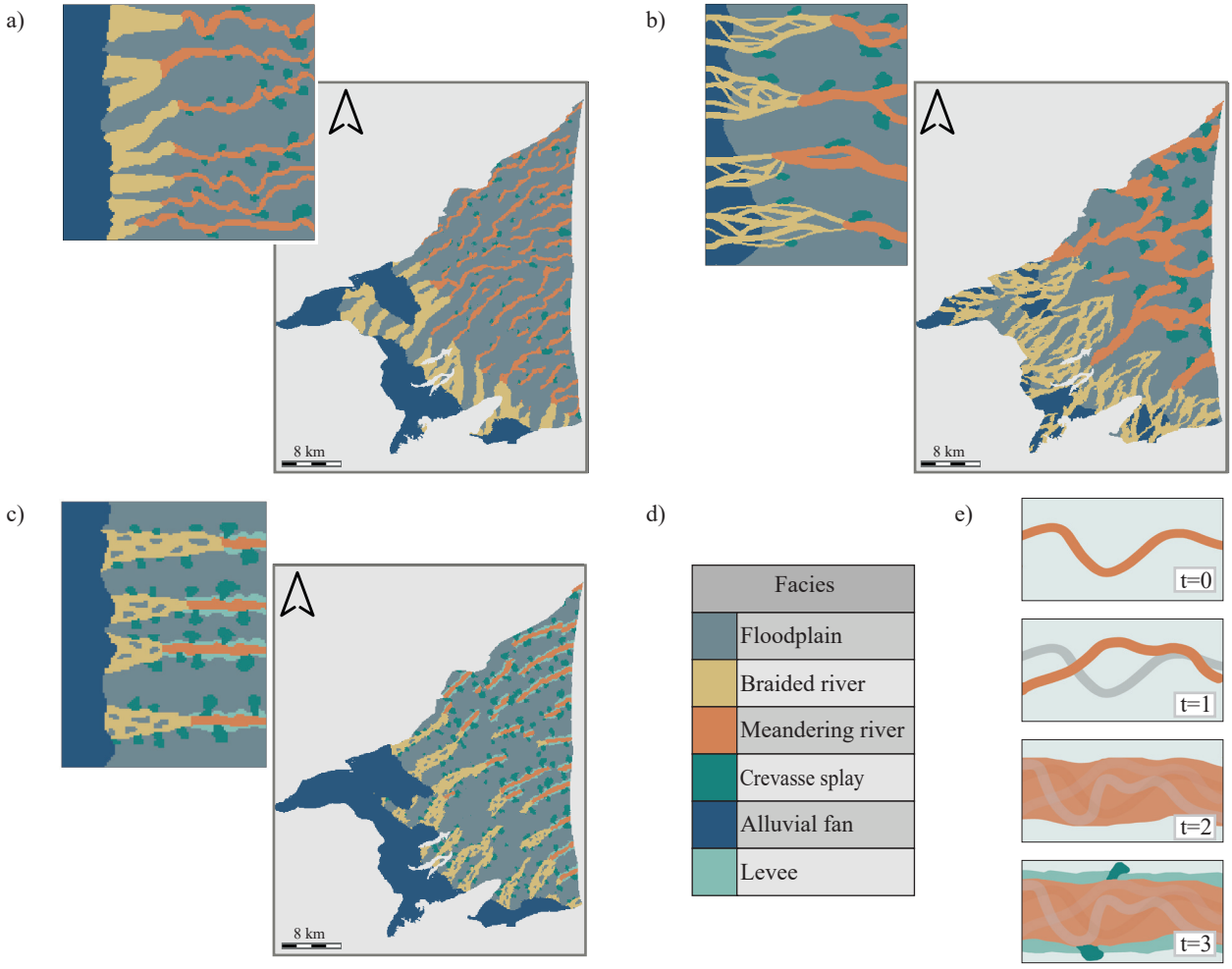

Figure 2. Horizontal TIs associated with their corresponding 2D MPS simulations. a) ~~an Italian analogue~~ analog TI derived from satellite images of the Tagliamento river, b) a conceptual analogue TI and c) a TI ~~created~~ creates based on outcrop ~~description~~ descriptions and general knowledge of the Roussillon's plain. d) the six sedimentary facies of the final TI. ~~d~~e) sedimentological concept for the creation of the final TI.

3.4 Flattened space simulation grid

With the creation of the TI, the conceptual sedimentation process of the Roussillon's plain is now transferred into ~~the~~ a model. The next step consists of creating a suitable simulation grid (SG) for the MPS simulation in accordance with the sedimentation process ~~express by~~ expressed in the TI. ~~It is thus~~ As mentioned before, it is decided to create the 3D model by staking 2D simulations in a transformed grid.

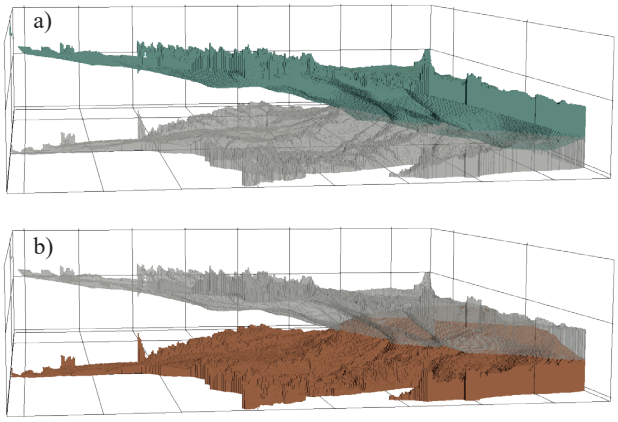

Figure 3. a) in dark green the 3D grid of the ~~PC layer~~ Pliocene (~~dark green~~the grey volume representing the transformed space). ~~e~~b) in dark orange the transformed grid (flattened space) of the ~~PC~~ Pliocene layer inside which the 2D simulations are simulated (~~dark orange~~the grey volume representing the original space). The vertical scale is exaggerated in this representation. View from the South of the area toward the North.

A regular cartesian grid is used for the simulation with the following dimensions: $407 \times 504 \times 125$ cells ($25'641'000$ cells in total) with a cell dimension of $100 \times 100 \times 2$ ~~m~~m. The z-axis dimension is defined in order to represent the minimal size of the sedimentary objects that we want to model while the x and y cell dimensions are defined to optimize the resolution of the modelled objects while keeping the computing time reasonable.

Digital elevation maps corresponding to the top and bottom altitudes of the ~~PC layer~~ Pliocene (Duvail, 2012) are used to select the active cells of the 3D simulation grid, the final volume of the ~~PC layer~~ Pliocene grid is composed of $3'753'230$ active cells (Fig. 3a). Since the TI represents the sedimentary evolution of a fluvial system, the 2D simulations have to be carried out in cells that share the same age of deposition. This requires to transform our 3D grid based on the topography of the bottom layer ~~of the PC~~ (Fig. 3b). A vertical shift is applied to each column of cells to flatten the base of the grid to the bottom of the Pliocene. With this transformation (flattened space), we create a 3D grid where it is possible to simulate inside horizontal layer z_i composed of cells sharing approximately the same age of deposition.

3.5 Trend Maps

In order to cope with the non-stationary TI, the model has to be constrained with one auxiliary variable map (trend map) for the TI and one for the simulation grid. For the TI, the trend map is simply the x coordinate re-scaled between 0 and 1 and corresponds to the lateral evolution of the fluvial system. This trend map has to be associated with ~~a~~ another trend map of similar range for the simulation grid.

Creating a 3D trend map for the ~~3D simulation grid~~ SG is complex due to the geometry of the ~~2D layers and therefore~~ layers and requires to develop a new approach, different from the one used for the TI. In the flattened space ~~simulation~~ grid, the auxiliary variable is computed by solving numerically a diffusivity equation ~~with proper boundary conditions in~~ in steady state ($\Delta h = 0$, with Δ representing the Laplacian operator) for each of the 2D ~~grid.~~ layer composing the 3D grid. The problem is solved using a finite element mesh following the exact geometry of the domain. The boundary conditions are: prescribed values $h(x) = h_0$ corresponding on some parts of the boundary; and $\nabla h(x) \cdot \boldsymbol{n}_x = 0$ on the rest, meaning that the gradient of $h(x)$ should be perpendicular to the vector $\boldsymbol{n}_x$ that is normal to the boundary at that location, i.e. the maximum variation of the trend must be parallel to the boundary. This problem is similar to the simulation of the hydraulic head in a homogeneous confined aquifer for a steady state flow. We associate the evolution of the hydraulic head between source zones (river input zones) and an outflow zone (the sea shore) and consider the result of the diffusivity equation (taking values between $[0, 1]$) as a proxy for describing the evolution of the sedimentary system in the SG (Fig. 4a). The four input zones correspond to the three main ~~paleo-rivers~~ paleo-river entrances and to the south relief zone where alluvial fan deposits are known to be present (Fig. 4a). The output zone corresponds to the seashore.

This approach is also ~~applied~~ used to create the vertical sedimentation trend of the plain, corresponding to the progradation of the sedimentary system towards the sea. By simulating 12 ~~different~~ representative 2D trend layers (Fig. 4 b) and combining them together vertically (assigning the first trend layer to the layers 0-9, the second trend layer to the layers 10-19 and so on), a complex 3D trend map is finally obtained. This trend map accounts for both vertical and lateral sedimentation trends that characterize the Roussillon's plain (Fig. 4c).

3.6 Rotation Maps

A 2D rotation map is created to control the orientation of the structures in the SG ~~, relative~~ relatively to their orientations in the TI. This map is built based on data gathered from field observations and interpretations of assumed rivers' paleo-orientations (Fig. 5a). The main river influx came from the Têt river in the central part of the basin and from the Tech river in the south-west part. Based on these orientations, a fictive rotation point set is created and interpolated using kriging.

The orientation map is based on interpretation and therefore uncertain. DeeSse allows to account for this uncertainty. A tolerance of +/- 10° is considered and added/subtracted to the kriged map to obtain two rotation maps: one with the minimal angle values and one with the maximal angle values (Fig. 5b).

The 3D maps are then created by extruding these rotation values along the z-axis, assuming that the variation of the paleo-orientations through time is encompassed within the tolerance values.

3.7 Vertical transition

To control the vertical transition from one layer to the next one, we developed a simple sampling approach, illustrated in Fig. 6. The approach starts by simulating the first layer of the transformed grid (layer 0/bottom layer) using only the borehole hard data set as conditioning data. Once this layer is simulated, points are sampled from this ~~simulated~~ layer and propagated as

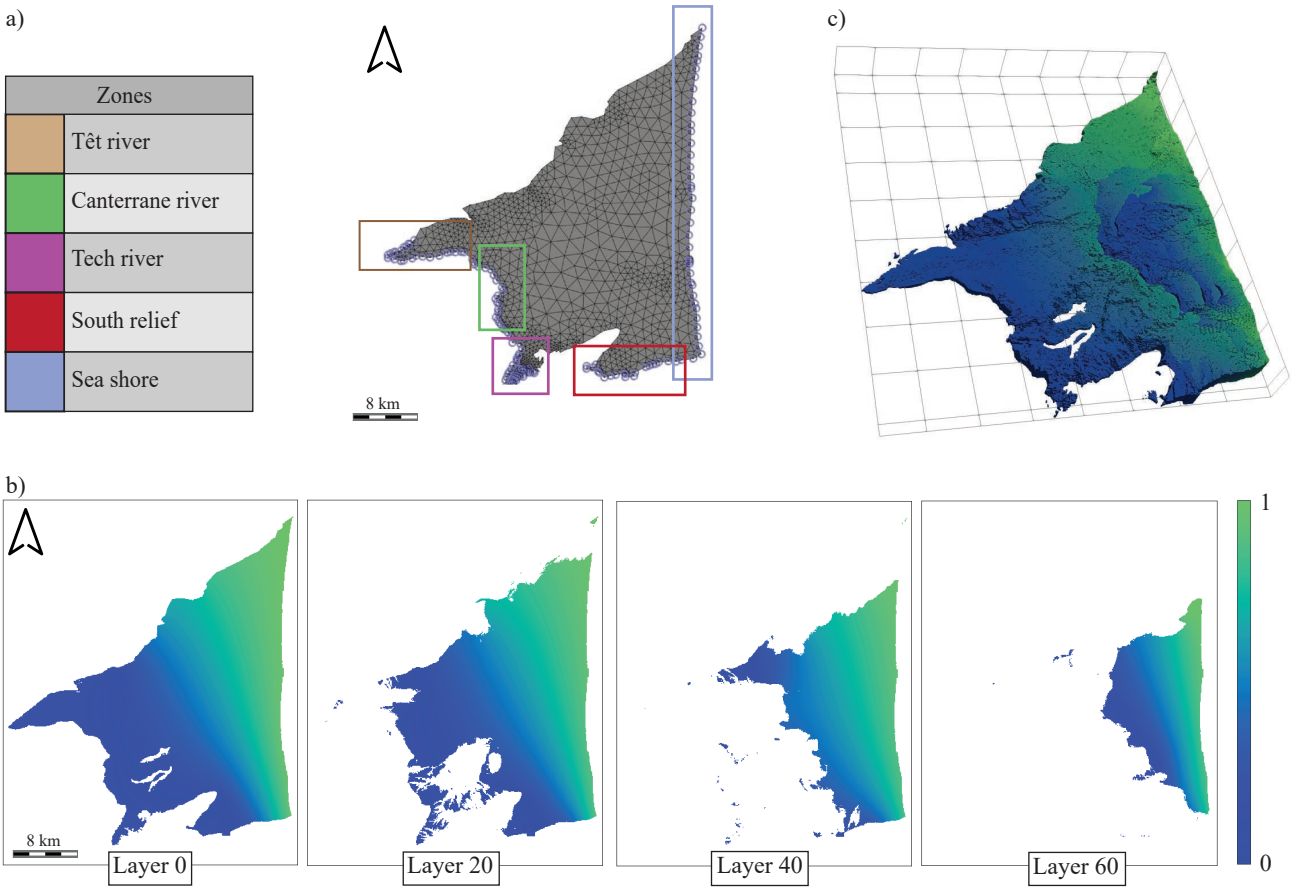

Figure 4. a) meshed grid with the four input zones and the one output zone used for the resolution of the diffusivity equation, b) different 2D layers that compose the 3D trend map of the transformed grid, c) top view of the 3D ~~(transformed/flattened)~~ trend map in the transformed space, where the progradation of the trend value towards the sea shore is visible.~~Both vertical and lateral trends of the PC are integrated to the 3D trend map.~~

additional (or secondary) hard data for the next layer. The facies value assigned to these points is drawn accordingly to the vertical transition probability between two facies, calculated from the boreholes hard data set.

Three parameters control this method, the first one defines which facies have to be sampled. ~~By default, all the facies can be sampled. However, after~~ After some tests, it ~~appeared that~~appears that, for the Roussillon case, the best way to control the vertical continuity ~~was~~ of the objects of interest is to sample only from three facies: the alluvial fan, the braided river and the ~~meander~~ meandering river facies. Since the floodplain facies is the most frequent one, sampling this facies at random location leads to an over-representation of the flood plain and tends to bias the MPS simulations. The levee and crevasse splay facies are not sampled in order to avoid to over constrain the structure of the fluvial objects. The second parameter is the sampling rate~~, it was fixed by trial and error at 1%~~. It is here fixed at 1 % of the number of simulated cells for each of the 3 facies.

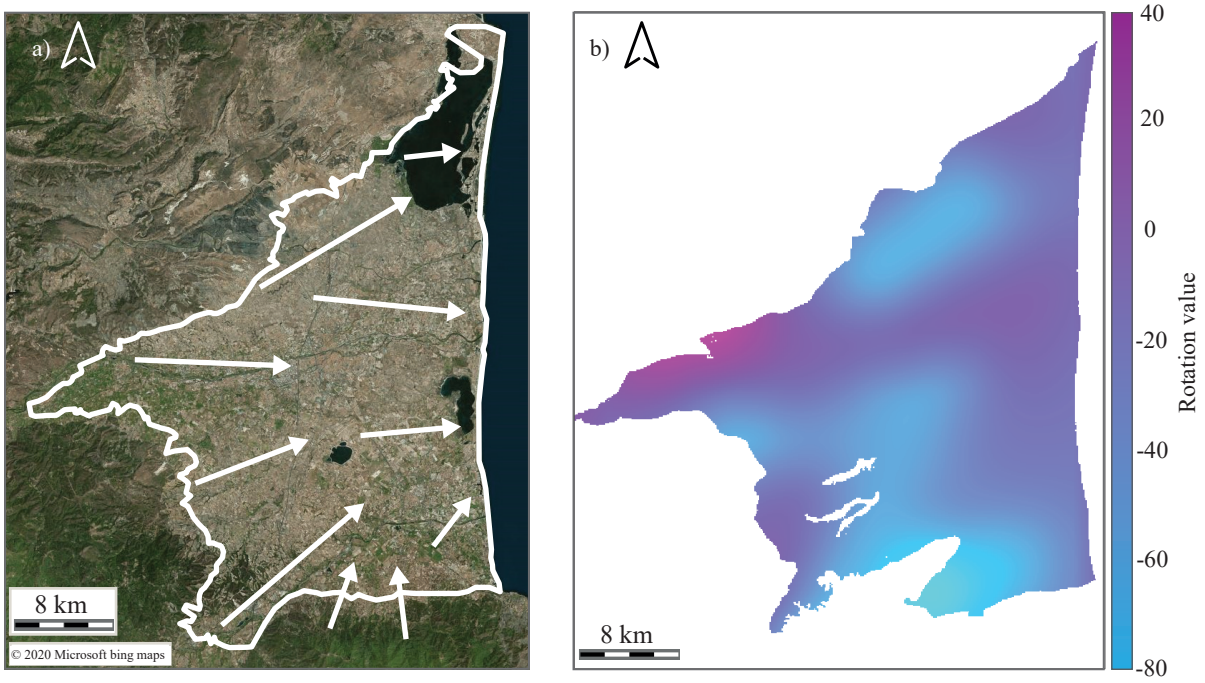

Figure 5. a) interpreted orientation of the paleo river in the Roussillon's plain~~,~~. b) interpolated continuous kriged values, where a positive rotation value corresponds to a clock-wise pattern rotation and and a negative rotation value corresponds to a anti-clock-wise pattern rotation.

The last parameter controls the maximum number of successive layers that are simulated using the sampling approach. This mechanism allows to control indirectly the maximal vertical size of the objects. This ~~parameter was~~ last parameter is set to 6 for the Roussillon case, meaning that after six successive layers simulated using the approach, the next ~~simulated layer~~ one will not use secondary sampled hard data.

Without this approach the vertical transition between facies would only be controlled by the hard conditioning data which are scarce compared to the size of the SG and the number of active cells that compose it.

3.8 DeeSse parameters

The main parameters used for the MPS simulation with DeeSse ~~were~~ are tested and chosen in order to minimize the simulation time without impairing the quality of the outputs. Two variables are considered: the facies (categorical) and the trend (continuous). The parameters defined for these two properties are the search ellipsoid which allows to limit the size of the pattern, the maximal number of pattern nodes (n)~~and~~, the acceptance threshold (t) and the scan fraction (f).

The search ellipsoids are identical for both variables and are defined by a radius of 20 cells in x and y axis directions and 0 along z because 2D simulations are performed. The maximal number of nodes is set to ~~$n = 24$~~ 24 for the facies variable and ~~set to $n = 5$~~ to 5 nodes for the trend variable. The larger number of neighboring nodes for the facies is defined to ensure a proper

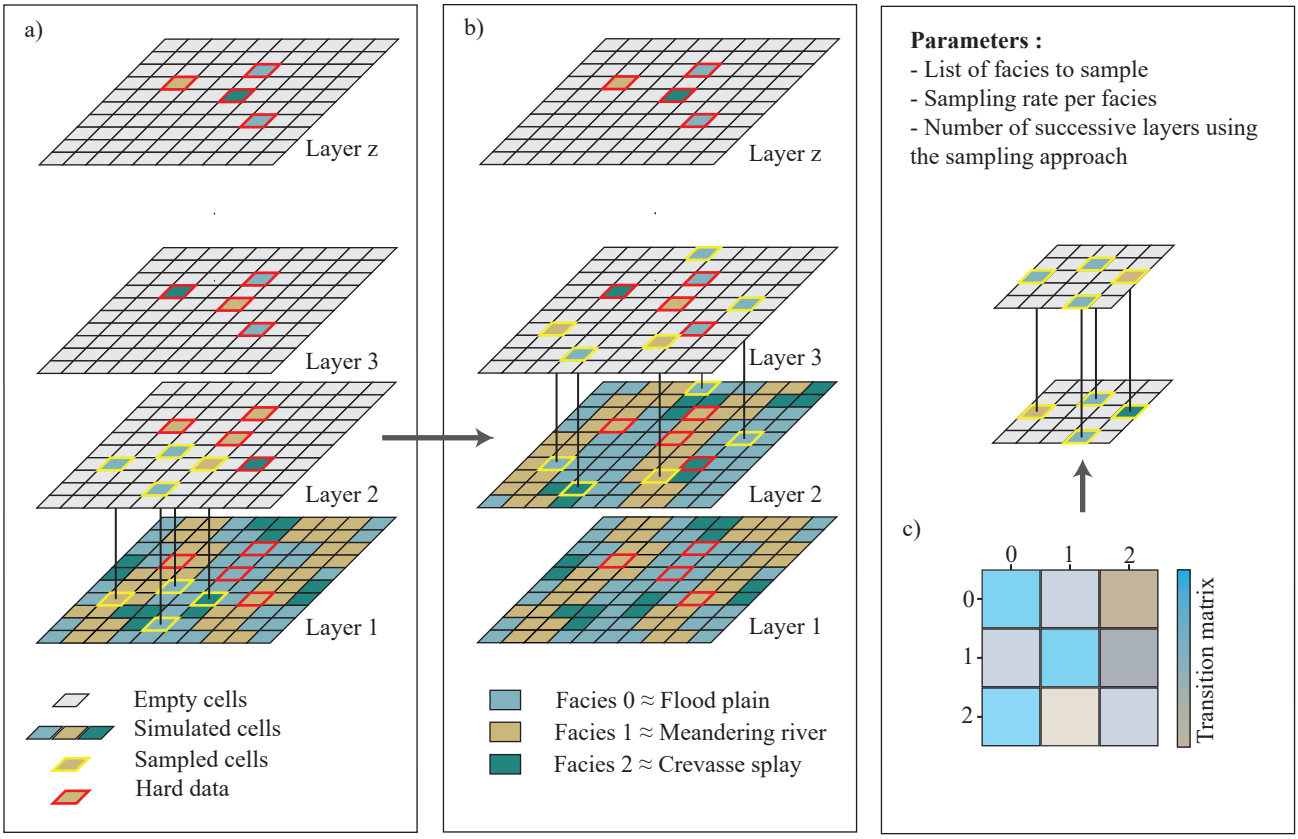

Figure 6. a) the first simulation takes place with only the hard data set as conditioning data. Then, a set of cells is sampled (in yellow) and used as new conditioning data for the next simulation. b) the process is repeated until the defined number of successive layers is reached. Once reached a simulation takes place without a sampling set. c) the value of the sampled cell is drawn based on the vertical transition matrix, calculated from the borehole data set.

pattern reproduction during the simulation at both large and fine scales. Since the trend variable is defined for every node of the SG, there is no need to define a large number of ~~pattern~~ nodes for that property. The threshold parameter t that controls the pattern quality reproduction is set to 0.05 for the facies property and to 0.25 for the trend property. Finally, the ~~maximal scanned fraction (f)~~ scanned fraction of the TI is set to 0.75.

Once satisfied with the 3D simulation output, the last step of the approach consists of producing a large number of simulations in order to compare them and to study the uncertainty of the model. The simulations are run on a CPU cluster, allowing to parallelize the computational load between different CPUs.

4 Simulation results

The following section presents the results of the workflow and the models obtained with DeeSse. The general aspect of the simulation is first discussed, before focusing on the ensemble statistics results calculated from 50 simulations sets.

Note that MPS validation is still an active research topic. Some tests and approaches are discussed for example by Mariethoz and Caers (2014). ~~Due~~ However, due to the small number of hard conditioning data, we limit ourselves in this work to analyse the plausibility of the geological patterns in the simulations with respect to the conceptual model, the final geological uncertainty resulting from the model, and some summary statistics.

4.1 3D simulation

One simulation is presented in Fig. 7. The first observation is that the model reproduces well the training image patterns over the different layers of the grid. All the main features of the TI are ~~well reproduced and not too disconnected~~ reproduced and the different patterns are globally not mixed between each others as it can be observed in the different horizontal-sections (Fig 7c) . Some discontinuities between the braided and ~~meander~~ meandering river deposits can be observed~~and are probably~~ . These discontinuities are due to the presence of hard conditioning data, which ~~doesn't~~ do not match the pattern locations imposed by the SG trend maps. The continuous rotation maps produce smooth pattern rotations, which could not be obtained with classical zonal rotation. ~~The use of continuous rotation maps~~ This feature helps to not break the pattern continuity and helps to create realistic ~~simulations~~simulated shapes.

Regarding the non-stationarity, we can see ~~in the 3D view (Fig. 7b)~~ that the simulated structures successfully follow the trend imposed by the auxiliary variable (Fig. 7c). In particular, the progradation trend imposed to the grid succeeds to reproduce a realistic vertical progradation of the system(Fig. 7b). The alluvial fans, which represents the start of the sedimentary system, gradually move toward the sea as the depth decreases in the model.

One 3D model, composed of $3'753'230$ active cells, is generated in about 15 min on a Intel®Core i7-7700 CPU at 3.6 GHz.

4.2 Probability Maps

Simulating a large number of realizations enables us to calculate probability maps (Fig. 8) and the pixel wise entropy of the simulations set (Fig. 9).

The probability maps display the probability of facies occurrence at each grid location based on 50 simulations (Fig. 8). If a facies is largely constrained at a spatial location, it is likely that all the simulations will simulate this facies at the same location and thus the probability map will display either very high or very low value at this spatial location. On the contrary, if a facies is less constrained, its probability map will display larger zones of occurrence through the simulations with more moderate values. The zones of extreme values are generally around hard conditioning data locations, which induce zones of low variability near them. These maps help the modeller to understand the model and the associated uncertainties. In this case we are focusing on the uncertainty regarding the shape of the channels and the uncertainty links to their spatial location.

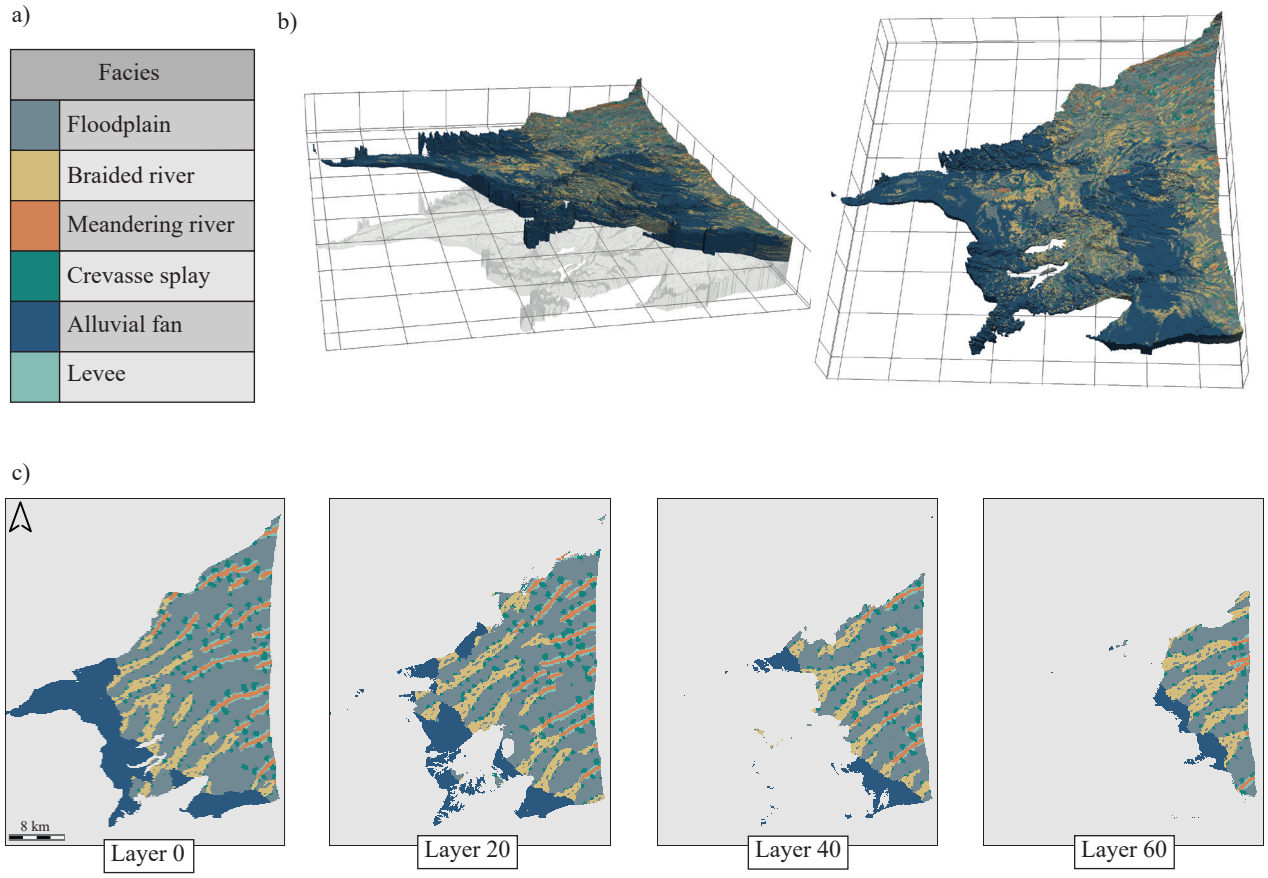

Figure 7. a) the 6 simulated facies, ~~e~~b) one 3D model of the simulations set, in the original 3D grid (left figure), and in the transformed grid (right figure). ~~b~~c) different z-layers (horizontal sections in the 3D transformed grid~~, where the 2D simulations are carried-on~~).

In Fig. 8, we can see that every facies has a different variability behaviour through the ensemble of simulation. However, the facies variability is not influenced by the depth of the simulated layer, every facies displaying the same probability range at different depths.

The alluvial fan facies is the more constrained of all of the simulated facies. It is mainly due to its low spatial variability imposed by the trend maps. The second most constrained facies ~~are the floodplaindeposit~~is the floodplain. It is mainly constrained by the other 5 facies, which explains its low variability in simulation. These high values are also linked to the dominance in proportion of this facies. For the braided river facies, the spatial probability of occurrence evolves through the layer and is mainly constrained by the hard data, creating zones of high probability. Moreover, the location of these facies are mainly controlled by the trend value of the simulation grid. The same observation can be transposed for the ~~meander~~ meandering river facies.

Finally, the crevasse splay deposits are homogeneously distributed through the layers and the levee facies is only simulated near the ~~meander river facies~~meandering river facies.

~~These probability maps, show that trend map has a strong influence on the patterns lateral location.~~ These maps also highlight the fact that the model is not over-constrained by ~~either the TI or the HDand reflect the uncertainties lying in our conceptual model~~ neither the TI nor the HD. Focusing on the meandering and braided river facies. We can observe that in some locations the probability maps show high probability values due to the presence of conditioning data. However, this probability decreases proportionally to the distance to the hard data, which demonstrates that the model is not over-constrained by the conditioning data. Moreover, even when a river bed location is constrained with a hard data, the associated spacing with other river bed is not fixed and can fluctuate through the simulation set, which indicates that the TI does not lock the locations of the pattern through the ensemble of simulations. Finally, this analyse of the simulations outputs is satisfying since it shows that the model respect the depositionnal concept expressed by the TI and the trend map.

4.3 Entropy Map

The six probability maps are used to calculate the information entropy. The Shannon Entropy was introduced in the theory of information developed by Shannon in the middle of the 20th century (Shannon, 1948) and represents the amount of information ~~that is included~~ carried within a probabilistic distribution. As proposed by Wellmann and Regenauer-lieb (2012), information entropy is an effective tool to visualize uncertainties in a spatial context. The main advantage of the entropy, is that it summaries the overall uncertainty contained in a probability distribution with a single number. The entropy is defined as:

$$H = -\sum_{i=1}^{n} p_i \log_n(p_i) \tag{1}$$

where n is the base of the logarithm corresponding to the number of categories (facies, 6 in our case) and p_i the probability of occurrence of the i-th category. The entropy is maximal and equal to 1 when all the outcomes have maximum uncertainty and is equal to 0 when there is a perfect certainty on the outcome.

The entropy map (Fig. 9) shows that there is little geological uncertainty in the upstream part of the plain where the alluvial fan ~~dominate~~dominates. Similarly, the uncertainty is rather small in the transition zone between braided and ~~meander~~ meandering river. The entropy map also reveals that the ~~meander~~ meandering river facies is mostly constrained ~~by~~ around the hard data~~, limiting its possible spatial locations in the simulation grid~~.

4.4 Facies proportion and vertical transition

Figure 10a compares the proportion of facies ~~of~~ from the TI, the hard conditioning data set and two ~~sets containing~~ simulation sets, each composed of 50 simulations~~each;~~ , the first one with the vertical sampling approach and the second one without it. Overall, the proportion ~~distributions~~ of simulated facies is ~~satisfying~~ satisfyingly reproduced when we compare the ~~simulation sets with~~ proportion distributions of the simulation sets against the proportion distribution of the hard data. It appears that the facies proportions are controlled by both the TI and hard data~~proportions~~, with the hard data set having a slightly larger

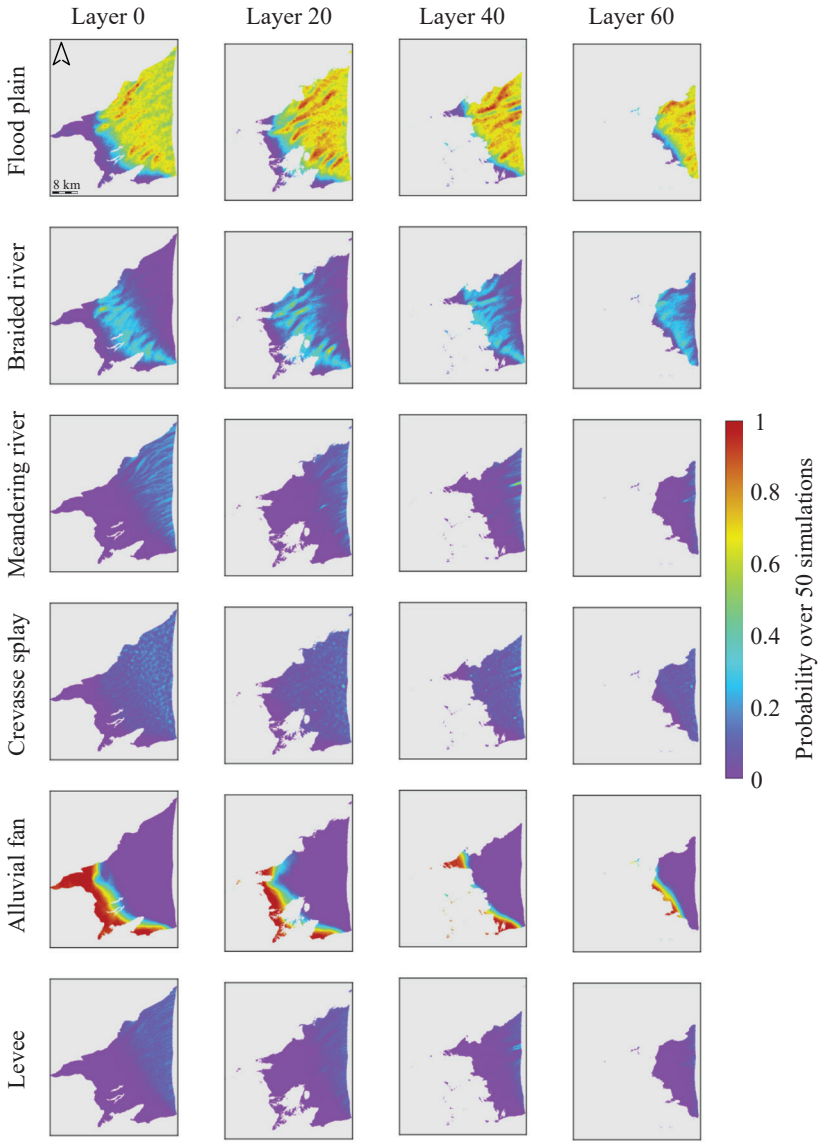

Figure 8. Probability maps of the 6 simulated facies at different depth. The probability maps are calculated over a 50 simulations set.

influence~~compare to the TI~~. This is reflected with the alluvial fan facies, which is less represented in the hard data set - mostly due to the central location on the plain of the majority of the boreholes - and less represented in the model compared to the TI proportion. ~~This facies percentage distribution shows~~ These facies proportion distributions show the importance of the hard data on the simulation output and the consequence that can ~~carry~~ arise from a biased hard data set.

To quantify the impact of the vertical sampling strategy~~on the simulations, we compare the vertical pixel-wise size distribution of the simulated object from the hard data set and the two simulation sets. To do so, a dissimilarity index is calculated for each~~

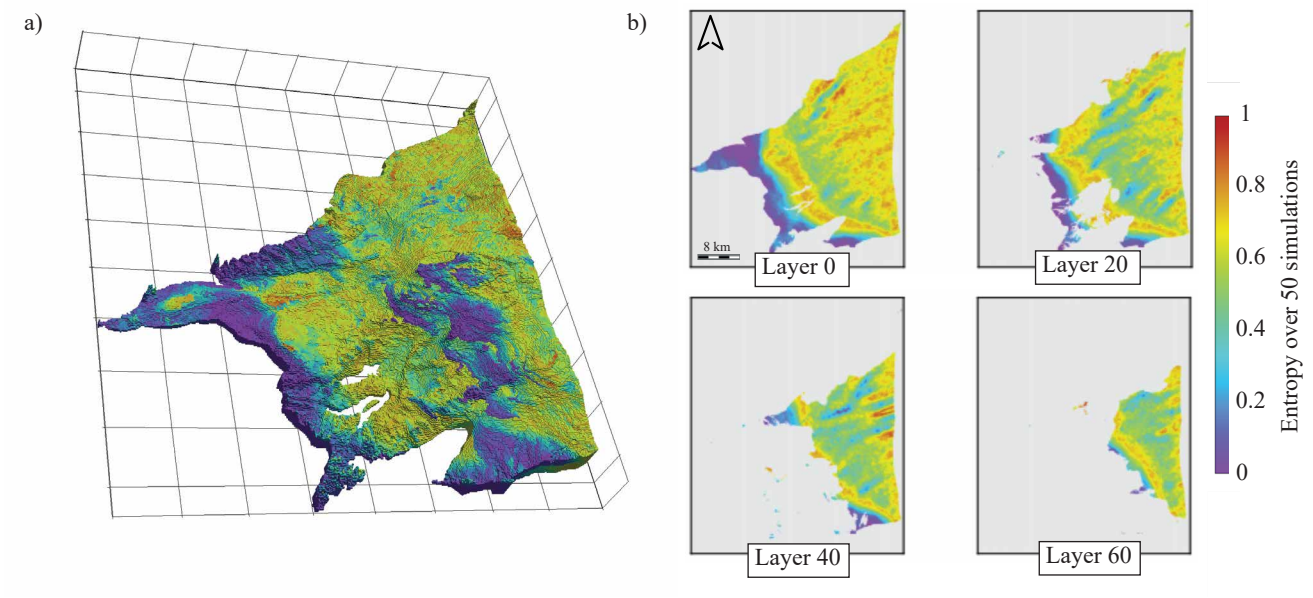

Figure 9. Shannon entropy of the model, calculated from the 6 facies probability maps. a) 3D views in the transformed grid, b) different z-layers (horizontal ~~2D layers within~~ sections in the 3D transformed grid).

~~simulated facies(Fig. 10b). This dissimilarity index quantifies the difference between two distributions, taking the vertical size distributions of the hard dataset as the reference distributions (the~~ , following previous authors, we compared the distributions of the vertical runs (Mood, 1940; Boisvert et al., 2007). To compute this indicator, the 3D grid is decomposed as a set of vertical columns of voxels. A vertical run is then defined as the length of a succession of the same facies values preceded and succeeded by a different facies. By computing the run length on all the columns for a given facies, one can compute the empirical distribution of runs for this facies. The same operation is conducted for all of the facies. In addition, these empirical distributions are also computed on the borehole data. We then compute dissimilarity indices between the simulated and observed distributions for all the facies using a normalized euclidean distance. The closest to zero the dissimilarity value is, the more identical the distributions are ~~). We use a normalized euclidean distance to calculate the index of dissimilarity~~and reciprocally (Fig. 10b). The alluvial fan facies is here not represented, because it is under-represented in the hard data set and a reference distribution cannot be inferred from it.

The impact of the sampling approach can also be observed when studying vertical cross-sections along the x and y axis in the transformed grid space (Fig. 11). In Fig. 11a the channels created by the stacking of the braided/meandering facies are vertically disconnected from each other. The sampling approach leads to the creation of vertically connected objects as can be observed in Fig. 11b. With this approach, "channels like" cross-sections can be observed in the simulation results while this was not the case before.

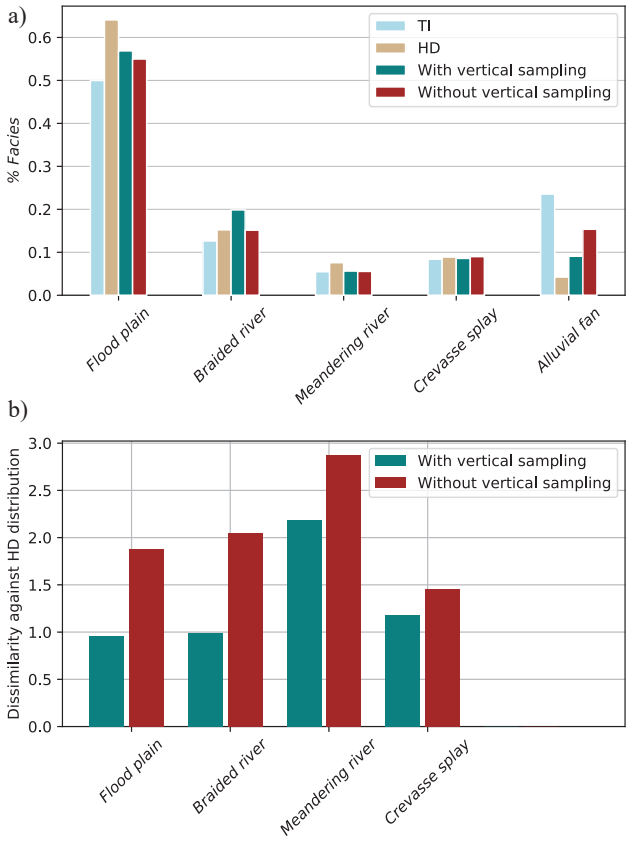

Figure 10. a) facies percentage in the training image, the hard data set, 3D simulation without vertical sampling and 3D simulation with vertical sampling. b) the dissimilarity values ~~for~~ of the two simulation sets. The dissimilarity ~~value is~~ values are calculated against the vertical size distribution of the hard conditioning data.

Overall, the simulation set using the vertical sampling strategy possesses distributions closer to the conditioning data (smaller dissimilarities value) and produces vertically connected objects. The set using the vertical sampling strategy is composed of a larger number of thick objects as compared to the simulations set not using the sampling approach. Figure 10b ~~shows~~ and Fig. 11b show the beneficial impact of the vertical sampling approach on the simulation outputs.

5 Discussion and ~~Conclusions~~Conclusion

This study proposes a new workflow for the simulation of complex heterogeneous ~~aquifer~~aquifers. Unlike more classical MPS studies, which rely on large primary or secondary hard data sets such as geophysics (Strebelle et al., 2002; Barfod et al., 2018; Høyer et al., 2017), this work relies on conceptual knowledge and auxiliary information.

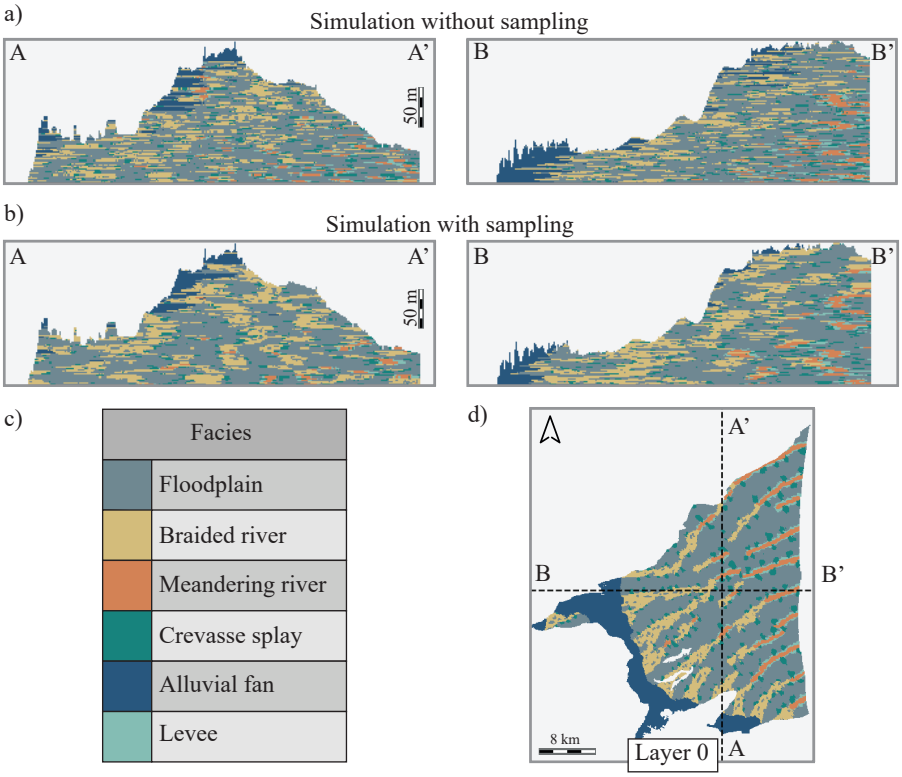

Figure 11. Cross-sections through two simulations, presented in the transformed space. a) two perpendicular vertical cross-sections through a simulation generated without the sampling approach. b) the same cross-sections through a simulation generated with the sampling approach. The braided and meandering facies display more vertical connection. d) Map view of the bottom layer of the simulation indicating the locations of the cross sections.

The main novelties within this workflow are the use of 2D simulations accounting for trends computed by solving a diffusion equation, the use of two continuous maps of rotation angles to account for the uncertainty on the paleo-orientations, and the transfer of conditioning data from layer to layer to constrain the vertical transitions between the facies.

Solving numerically the diffusion equation allows to account easily for the complex geometry of the extension of the sedimentary basin when computing the trend map. Using that technique, it is straightforward to impose prescribed values of the trend on certain parts of the boundary and to ensure that the gradient of the trend will remain perpendicular to the sides of the domain.

The proposed approach is simpler and faster than one based on ~~a~~ 3D TI. It has the advantage of being more flexible during the development of the model, where all of the elements can be easily adapted to the specific case and tested. In particular, the possibility of using auxiliary information allows the modeller to approach each problem with a different angle making MPS, and especially DeeSse very flexible.

The study of the Roussillon plain shows the importance of testing different TIs to obtain acceptable structures. The TI must be created to reflect the general geological knowledge available for the study site and it must respect the interpreted data. One of the strengths of the MPS method is that it allows to test rapidly different concepts that can be discussed and adapted. Moreover, the use of complex auxiliary variable and continuous rotation maps allow the final model to account for that information while honoring the borehole data.

The robustness of the proposed methodology has been tested with two sets of 50 simulations, one set with the vertical sampling approach and the other one without it. Despite its relatively simple method, the vertical sampling improves the vertical object' size reproduction. The simulation without vertical sampling misses to create the large vertically connected objects, where the simulations with vertical sampling have a distribution more comparable to the hard data set distribution (Fig. 10b). These improvements, regarding the vertical objects size reproduction, are important, since the ~~meander~~ meandering river deposits and the braided river deposits are known to have high aquifer potentials. Recreating the vertical connectivity of these objects is a key parameter for the future use of the geological model for the hydro-characterization of the aquifer.

The probability and the entropy maps show that the important sedimentary concepts have been well integrated into the model. The facies proportion ~~distribution~~ distributions of the different objects ~~is~~ are satisfactorily reproduced and ~~is~~ are constrained by both the boreholes facies distribution and the TI distribution. The probability and the entropy maps also show a lack of hard data. Indeed, the hard data set used may not be fully representative of the facies distribution of the ~~PC aquifer~~ Pliocene and the simulation can suffer from this bias. Regarding the vertical sampling approach, even if it improves the realism of the simulated object, the simulated shapes would benefit from additional constraints. The vertical transition matrix inferred from the boreholes can also present a bias due to their location or their non-representativeness of the real transition matrix.

Therefore, the model of the Roussillon plain would clearly benefit from additional boreholes with gamma ray and resistivity logs at locations that are not yet constrained. A denser data set would permit to conduct a meaningful cross validation exercise as suggested by Juda et al. (2020). At present, the data are not sufficient to really test carefully the predictive power of the MPS model. The model of the Roussillon plain would also benefit from additional information regarding the geometry of the sedimentological objects (their width, their lateral distribution...). Analogue data or geophysical inputs could help to better understand these geometries and could help in characterizing the transition zone between braided and ~~meander river~~ meandering river deposits.

Finally, despite these possible improvements, this work demonstrates the applicability of DeeSse and of the proposed workflow to simulate complex internal aquifer heterogeneity at a regional scale.

Author contributions. AUTHOR CONTRIBUTION

V. Dall'Alba developed and coded the workflow, interpreted the geophysical logs, discussed the conceptual geological model, conducted all the numerical experiments, produced the figures and wrote the article. C. Duvail and B. Issautier developed the conceptual geological model and helped for the geophysical logs interpretation. J. Straubhaar and P. Renard supervised the research and in particular the design of the workflow and provided guidance for the MPS simulations. Y. Caballero coordinated

the whole project, and contributed to the hydrogeology section of this paper. Finally, all authors have helped during the writing process of this paper.

Competing interests. COMPETING INTERESTS

The authors declare that they have no conflict of interest.

Acknowledgements. The authors thank the ~~different~~ partners of the Dem'Eaux Roussillon project and the University of Neuchâtel for supporting the development of this work.

References

Aunay, B., Duvail, C., Giordana, G., Doerfliger, N., Le Strat, P., Montginoul, M., and Pistre, S.: A pluridisciplinary methodology for integrated management of a coastal aquifer: Geological, hydrogeological and economic studies of the Roussillon aquifer (Pyrénées-Orientales, France), Vie et Milieu, 56, 2006.

Barfod, A. A., Møller, I., Christiansen, A. V., Hoyer, A. S., Hoffimann, J., Straubhaar, J., and Caers, J.: Hydrostratigraphic modeling using multiple-point statistics and airborne transient electromagnetic methods, Hydrology and Earth System Sciences, 22, 3351–3373, https://doi.org/10.5194/hess-22-3351-2018, 2018.

Boisvert, J. B., Pyrcz, M. J., and Deutsch, C. V.: Multiple-point statistics for training image selection, Natural Resources Research, 16, 313–321, 2007.

Caballero, Y. and Ladouche, B.: Impact of climate change on groundwater in a confined Mediterranean aquifer, Hydrology and Earth System Sciences Discussions, 12, 10 109–10 156, 2015.

Chauveau, M., Chazot, S., Perrin, C., Bourgin, P.-Y., Sauquet, E., Vidal, J.-P., Rouchy, N., Martin, E., David, J., Norotte, T., Maugis, P., and De Lacaze, X.: Quels impacts des changements climatiques sur les eaux de surface en France à l'horizon 2070 ?, La Houille Blanche, pp. 5–15, https://doi.org/10.1051/lhb/2013027, 2013.

Chugunova, T. and Hu, L.: Multiple-Point simulations constrained by continuous auxiliary data, Mathematical Geosciences, 40, 133–146, https://doi.org/10.1007/s11004-007-9142-4, 2008.

Clauzon, G., Le Strat, P., Duvail, C., Do Couto, D., Suc, J. P., Molliex, S., Bache, F., Besson, D., Lindsay, E. H., Opdyke, N. D., Rubino, J. L., Popescu, S. M., Haq, B. U., and Gorini, C.: The Roussillon Basin (S. France): A case-study to distinguish local and regional events between 6 and 3 Ma, Marine and Petroleum Geology, 66, 18–40, https://doi.org/10.1016/j.marpetgeo.2015.03.012, 2015.

Colombera, L., Felletti, F., Mountney, N. P., and McCaffrey, W. D.: A database approach for constraining stochastic simulations of the sedimentary heterogeneity of fluvial reservoirs, AAPG bulletin, 96, 2143–2166, 2012.

Comunian, A., Renard, P., and Straubhaar, J.: 3D multiple-point statistics simulation using 2D training images, Computers & Geosciences, 40, 49–65, 2012.

Cordua, K. S., Hansen, T. M., Gulbrandsen, M. L., Barnes, C., and Mosegaard, K.: Mixed-point geostatistical simulation: A combination of two-and multiple-point geostatistics, Geophysical Research Letters, 43, 9030–9037, 2016.

de Carvalho, P. R. M., da Costa, J. F. C. L., Rasera, L. G., and Varella, L. E. S.: Geostatistical facies simulation with geometric patterns of a petroleum reservoir, Stochastic Environmental Research and Risk Assessment, 31, 1805–1822, https://doi.org/10.1007/s00477-016-1243-5, 2017.

de Marsily, G., Delay, F., Gonçalvès, J., Renard, P., Teles, V., and Violette, S.: Dealing with spatial heterogeneity, Hydrogeology Journal, 13, 161–183, 2005.

Duvail, C.: Expression des facteurs régionaux et locaux dans l'enregistrement sédimentaire d'une marge passive. Exemple de la marge du Golfe du Lion, étudiée selon un continuum terre-mer., Université de Montpellier 2, https://doi.org/tel-00438146, 2008.

Duvail, C.: Caractérisation de la géométrie et de l ' architecture des formations du Pliocène de la plaine du Roussillon pour la modélisation hydrodynamique., Tech. rep., BRGM, Geoter, 2012.

Duvail, C., Gorini, C., Lofi, J., Le Strat, P., Clauzon, G., and dos Reis, A. T.: Correlation between onshore and offshore Pliocene-Quaternary systems tracts below the Roussillon Basin (eastern Pyrenees, France), Marine and Petroleum Geology, 22, 747–756, 2005.

Genna, A.: Carte géologique harmonisée du département des Pyrénées-Orientales. Notice technique. Rapport final. RP-57032FR, Tech. rep., BRGM, 2009.

Hoffimann, J., Scheidt, C., Barfod, A., and Caers, J.: Stochastic simulation by image quilting of process-based geological models, Computers & Geosciences, 106, 18–32, https://doi.org/10.1016/j.cageo.2017.05.012, https://doi.org/10.1016/j.cageo.2017.05.012, 2017.

Høyer, A. S., Vignoli, G., Hansen, T. M., Vu, L. T., Keefer, D. A., and Jørgensen, F.: Multiple-point statistical simulation for hydrogeological models: 3-D training image development and conditioning strategies, Hydrology and Earth System Sciences, 21, 6069–6089, https://doi.org/10.5194/hess-21-6069-2017, 2017.

Hu, L. Y. and Chugunova, T.: Multiple-point geostatistics for modeling subsurface heterogeneity: A comprehensive review, Water Resources Research, 44, 1–14, https://doi.org/10.1029/2008WR006993, 2008.

Journel, A. G.: Geostatistics for Conditional Simulation of Ore Bodies, Economic Geology, 69, 673–687, https://doi.org/10.2113/gsecongeo.69.5.673, 1974.

Juda, P., Renard, P., and Straubhaar, J.: A framework for the cross-validation of categorical geostatistical simulations, Earth and Space Science, https://doi.org/10.1029/2020ea001152, https://doi.org/10.1029/2020ea001152, 2020.

Koltermann, C. E. and Gorelick, S. M.: Heterogeneity in sedimentary deposits: A review of structure-imitating, process-imitating, and descriptive approaches, Water Resources Research, 32, 2617–2658, 1996.

Lofi, J., Gorini, C., Berné, S., Clauzon, G., Dos Reis, A. T., Ryan, W. B., and Steckler, M. S.: Erosional processes and paleoenvironmental changes in the Western Gulf of Lions (SW France) during the Messinian Salinity Crisis, Marine Geology, 217, 1–30, https://doi.org/10.1016/j.margeo.2005.02.014, 2005.

Mariethoz, G. and Caers, J.: Multiple-Point Geostatistics: stochastic modeling with training images, Wiley-Blackwell. A John wiley and Sons, LTD, Publication, 2014.

Mariethoz, G., Renard, P., and Straubhaar, J.: The direct sampling method to perform multiple-point geostatistical simulations, Water Resources Research, 46, 1–14, https://doi.org/10.1029/2008WR007621, 2010.

Matheron, G.: Principles of geostatistics, Economic Geology, 58, 1246–1266, https://doi.org/10.2113/gsecongeo.58.8.1246, 1963.

Matheron, G., Beucher, H., De Fouquet, C., Galli, A., Guerillot, D., Ravenne, C., et al.: Conditional simulation of the geometry of fluvio-deltaic reservoirs, Society of Petroleum Engineers, 1987.

Meerschman, E., Pirot, G., Mariethoz, G., Straubhaar, J., Van Meirvenne, M., and Renard, P.: A practical guide to performing multiple-point statistical simulations with the Direct Sampling algorithm, Computers and Geosciences, 52, 307–324, https://doi.org/10.1016/j.cageo.2012.09.019, 2013.

Mood, A. M.: The distribution theory of runs, The Annals of Mathematical Statistics, 11, 367–392, 1940.

Naranjo-Fernández, N., Guardiola-Albert, C., and Montero-González, E.: Applying 3D geostatistical simulation to improve the groundwater management modelling of sedimentary aquifers: The case of Doñana (Southwest Spain), Water (Switzerland), 11, https://doi.org/10.3390/w11010039, 2018.

Nichols, G. J. and Fisher, J. A.: Processes, facies and architecture of fluvial distributary system deposits, Sedimentary Geology, 195, 75–90, https://doi.org/10.1016/j.sedgeo.2006.07.004, 2007.

Serra O., S. L. et al.: Sedimentological analysis of shale-sand series from well logs, Society of Petrophysicists and Well-Log Analysts, 1975.

Shannon, C. E.: A Mathematical Theory of Communication, Bell System Technical Journal, 5, https://doi.org/10.1002/j.1538-7305.1948.tb01338.x, 1948.

Straubhaar, J.: DeeSse user's guide, Tech. rep., The Centre for Hydrogeology and Geothermics (CHYN), University of Neuchâtel: Neuchâtel, Switzerland, 2019.

Straubhaar, J., Renard, P., Mariethoz, G., Froidevaux, R., and Besson, O.: An improved parallel multiple-point algorithm using a list approach, Mathematical Geosciences, 43, 305–328, https://doi.org/10.1007/s11004-011-9328-7, 2011.

Straubhaar, J., Walgenwitz, A., and Renard, P.: Parallel Multiple-Point Statistics Algorithm Based on List and Tree Structures, Mathematical Geosciences, 45, 131–147, https://doi.org/10.1007/s11004-012-9437-y, 2013.

Straubhaar, J., Renard, P., and Mariethoz, G.: Conditioning multiple-point statistics simulations to block data, Spatial Statistics, 16, 53–71, 2016.

Straubhaar, J., Renard, P., and Chugunova, T.: Multiple-point statistics using multi-resolution images, Stochastic Environmental Research and Risk Assessment, pp. 1–23, 2020.

Strebelle, S., Payrazyan, K., and Caers, J.: Modeling of a Deepwater Turbidite Reservoir Conditional to Seismic Data Using Multiple-Point Geostatistics, SPE Annual Technical Conference and Exhibition, https://doi.org/10.2118/77425-MS, 2002.

Tahmasebi, P., Hezarkhani, A., and Sahimi, M.: Multiple-point geostatistical modeling based on the cross-correlation functions, Computational Geosciences, 16, 779–797, https://doi.org/10.1007/s10596-012-9287-1, 2012.

Wellmann, J. F. and Regenauer-lieb, K.: Uncertainties have a meaning : Information entropy as a quality measure for 3-D geological models, Tectonophysics, 526-529, 207–216, https://doi.org/10.1016/j.tecto.2011.05.001, 2012.

Zhang, T., Switzer, P., and Journel, A.: Filter-based classification of training image patterns for spatial simulation, Mathematical Geology, 38, 63–80, https://doi.org/10.1007/s11004-005-9004-x, 2006.